Surface and quantum-size effects in Pt and Au nanoparticles probed by ^197Au Mössbauer effect spectroscopy

Paulus, P.M.; Goossens, A.; Thiel, R.C.; Kraan, A.M. van der; Schmid, G.; Jongh, L.J. de

Surface and quantum-size effects in Pt and Au nanoparticles probed by ^{197}Au Mössbauer spectroscopy

P. M. Paulus,[1] A. Goossens,[1,2] R. C. Thiel,[1] A. M. van der Kraan,[2] G. Schmid,[3] and L. J. de Jongh[1,*]
[1]*Kamerlingh Onnes Laboratorium, Universiteit Leiden, P. O. Box 9504, 2300 RA Leiden, The Netherlands*
[2]*Interfacultair Reactor Instituut, Delft University of Technology, Mekelweg 15, 2629 JB Delft, The Netherlands*
[3]*Institut für Anorganische Chemie, Universität Essen, Universitätsstrasse 5–7, D-45117 Essen, Germany*
(Received 20 December 2000; revised manuscript received 1 June 2001; published 6 November 2001)

Molecular metal nanoclusters and metal colloids are attractive systems to study surface and quantum-size effects on conduction electrons and phonons. Mössbauer spectroscopy is an excellent tool to study such phenomena. We present a detailed analysis of ^{197}Au Mössbauer spectra taken from a series of Au and Pt nanoparticles of sizes 1–17 nm. A central force model with only nearest-neighbor interactions gives a satisfactory description of the recoil-free fractions. A site-dependent local density-of-states approach is used to describe the surface and size effects on the electronic properties of the nanoparticles, as reflected in the Mössbauer isomer shifts and quadrupole splittings. A correlation of these parameters with the location of the site on the cluster surface is found. We conclude that, even for ligated metal clusters, the surface-atomic layer has predominantly ''metallic'' character, in the sense that it is a part of the total volume over which the electrons are delocalized, so that free charge exchange is possible between surface atoms and the inner core of the particle. For the smaller particles, the electron density is found to vary throughout the metal core, which is interpreted in terms of surface screening and quantum-size effects.

DOI: 10.1103/PhysRevB.64.205418 PACS number(s): 73.21.−b, 63.22.+m, 33.45.+x, 61.46.+w

I. INTRODUCTION

Small metal particles, having a diameter down to a nanometer, are attractive subjects of both fundamental and technological research. Due to their large surface-to-volume ratio, they present ideal systems to study surface effects on the conduction electrons. Furthermore, as the size of the particles decreases to values comparable to the wavelength of an electron at the Fermi energy (about 1 nm for a metal), quantum-size effects will occur, due to the extreme confinement of the electrons. In this paper, we investigate the effects of the surface and of molecules bonded to it, besides the phenomena resulting from the small particle size. Mössbauer spectroscopy proves to be an excellent tool to study such size effects, since it is an *element selective* and *local* probe, providing information on different sites within the particle separately. In addition, size effects on the lattice vibrations can be observed. However, to obtain clear information, it is of crucial importance to avoid the need to average over size distributions, implying that all particles should have the same size, or at least nearly so. Fortunately, in the last decade, chemists have been able to prepare stoichiometric molecular cluster compounds that meet this requirement very well.[1,2] They are composed of molecular metal clusters, stabilized by ligand molecules and atoms, which prevent the clusters from coalescing. In these compounds, all molecules are in principle identical and thus all clusters should have the same size, apart from possible deviations from stoichiometry, as may occur in such complex chemical compounds. In this work, we focus on a special class of these materials, the so-called magic number metal cluster molecules, as synthesized in recent years by Schmid and co-workers.[1] In these molecules, the metal cores (clusters) are composed of a central metal atom, surrounded by a number of successive full shells of metal atoms in fcc packing [as evidenced by extended x-ray-absorption fine-structure (EXAFS) and x-ray investigations[3–5]]. This results in clusters with 13, 55, 147, 309, etc. atoms per particle, corresponding to one, two, three, four, etc. full shells, respectively. Schmid *et al.*[1,2] have prepared a series of Pt, Au, and Pd clusters of varying sizes, namely, Au2, Pt2, Pt4, Pd2, Pd4, Pd5, Pd7, and Pd8, where the number refers to the number of full shells of atoms.[6] Some of these could be synthesized with different ligands, giving the opportunity to study the effect of the ligands on the properties of the particles.[1,2,6] Using similar ligands, also colloidal substances consisting of larger metal particles, have been synthesized by Schmid and coworkers, albeit with a small distribution in size (5–15 %). These colloidal particles provide an attractive intermediate between the molecular clusters and the bulk metals, and will be indicated as M-c#. This designates a colloid of metal atoms of type M, and an average diameter of # Å . We will also report on a carbonyl-stabilized Pt_{38} molecular cluster, synthesized by Ceriotti *et al.*[7] We remark that a previous Mössbauer study on large Au colloidal particles has been made by Viegers and Trooster.[8] Recently a renewed interest in Au particles has arisen because of their catalytic properties.[9,10]

In recent years, an extensive study of the size evolution of the physical (thermodynamic) properties of the above metal cluster compounds has been made, in particular on the Pd series.[11] In addition, several publications have appeared on the effects of ligand bonding on the electronic and vibrational properties of the clusters.[12–15] Here we shall present a detailed analysis of a number of Mössbauer spectra, in combination with a reanalysis of previously published data. As will be shown, all Mössbauer data on the vibrational properties of the atoms within the clusters can be interpreted in a way consistent with results derived from specific-heat and

EXAFS experiments. For instance, in the Au2 clusters, a lattice contraction was previously observed from EXAFS,[16] with a simultaneous stiffening of the lattice.[14] This is supported by the present analysis of the Mössbauer recoilless fractions (f factors). In the Pt4 clusters, no appreciable lattice contraction was observed from EXAFS.[17] The f factors in Pt4 and Pt2 clusters can indeed be modeled on this basis, using interatomic force parameters derived from bulk properties.

Surface and quantum-size effects (QSE) on the electronic properties of the clusters have already been evidenced in earlier work, namely, in combined low temperature ($T < 1$ K) specific-heat and magnetic-susceptibility measurements on the above-mentioned series of Pd clusters,[18] and in an extensive NMR study of a Pt4 cluster.[19] However, until now our published Mössbauer data on Au and Pt clusters[15,20–23] did not show clear indications of these effects, except for the metal atoms in the outermost layer, where the surface and the ligands influence the local coordination, site symmetry, and charge density. With the data presented here, we are able to show that the combination of Mössbauer spectra of the series of Au and Pt clusters clearly exhibits features that can be well explained in terms of an electronic local density of states which varies throughout the core of the particles. This interpretation is analogous to that previously used to explain the NMR data on Pt catalysts[24] and, more recently, on Pt4phen* (phen* is the 1,10-phenanthroline derivative).[19] As we shall argue, such a variation can be caused by the effect of surface screening, or may result from the QSE, or from a combination of both.

In addition, we shall discuss the correlations of the Mössbauer parameters for the different Au sites at the surface of the clusters, with their nearest-neighbor coordination formed by other metal atoms and ligands. On the one hand, if we assume that the surface metal-atom layer is *''metallic,'' by which we shall mean that it is part of the total volume over which the electrons are delocalized in the particle*, a narrowing of the 5d bands is expected at the surface (cf. Sec. III). This will cause a variation of Mössbauer parameters, depending on the local surrounding of metal atoms at each surface site. On the other hand, a large fraction of the surface atoms is bonded to ligands, which are adsorbed onto the metal particles. If the bonding with the ligands would render the surface layer ''nonmetallic,'' i.e., the surface Au atoms would be charged to definite valence states, a correlation may emerge between the Mössbauer parameters of a surface site and the type of ligand bonded to it, similar to the correlations found for monatomic Au complexes.[25–28] In those compounds, the Au atoms have a definite valency and a local symmetry, which is determined by the ligand coordination.

A rigorous theoretical treatment of the electronic structure in transition-metal particles is very difficult, except for the smallest ones, containing only a few atoms. Local density-functional calculations indicate that the electronic structure can strongly deviate from that in the bulk.[12,13,29] For example, in ligated transition-metal clusters, the number of electrons in surface-atom s orbitals decreases in favor of that in d and p orbitals.[13,30] The values of electric-field gradients and electron densities are very sensitive to these kinds of changes, resulting in variations of the Mössbauer parameters. In principle, these types of calculations could give us quantitative values for these Mössbauer parameters at the various sites. However, since we are also dealing with particles larger than can be handled in a rigorous treatment, we will in addition have to use a more qualitative approach to explain the observed trends in the physical properties. For this, we shall use general conclusions that can be drawn from jellium-model calculations and tight-binding theory for surfaces and particles.

TABLE I. Compilation of the investigated samples with the abbreviations as used throughout the article. The number in the abbreviation of the magic number clusters indicates the number of full shells of atoms surrounding a single central atom. Abbreviations M-c# designate M colloids with an average diameter of # Å . See Fig. 2 for a drawing of the two- and four-shell clusters, Fig. 1 for the full molecular structure of Pt_{38}, and Fig. 3 for a drawing of PPh_3 (triphenylphosphine), phen* (1,10-phenanthroline derivative), and cinc (cinchonidine). PNS is $C_6H_6NNaSO_3S\cdot 2H_2O$, Bu is a butyl radical, HAc an acetate molecule: CH_3COOH, TSTPP is a trisulfunated PPh_3, and MSTPP is a monosulfunated PPh_3. The last column gives the average diameter of the metal core of the particles. The number of metal atoms in the Pt-c33 particles is based on a Pt6 geometry (see text), whereas those in the Au colloids are derived from their average volumes.

Chemical formula	Abbreviation	$\langle\varnothing\rangle$ (nm)
$Pt_{309}phen^{*}_{36}O_{30\pm 10}$	Pt4phen*	2.1
$Pt_{309}cinc_{102}(HAc)_{369}$	Pt4cinc	2.1
$t_{923\pm 150}(PNS)_N$	Pt-c33	3.3 ± 0.2
$Au_{157000\pm 26000}(TSTPP)_M$	Au-c172	17.2 ± 0.9
$Au_{8900\pm 2400}(MSTPP)_{M'}$	Au-c66	6.6 ± 0.6
$Au_{8500\pm 3900}(MSTPP)_{M''}$	Au-c65	6.5 ± 1.0
$Au_{55}(PPh_3)_{12}Cl_6$	Au2tpp	1.2
$Pt_{55}(AsBu_3)_{12}Cl_{20}$	Pt2	1.2
$[Pt_{38}(CO)_{44}](PPh_4)_2$	Pt_{38}	0.9

The outline of this paper is as follows. In the next section, a number of experimental details is presented. This is followed by a more detailed inspection of the surface and size effects on the Mössbauer parameters in nanoparticles, with respect to their electronic properties (Sec. III), and with respect to their vibrational properties (Sec. IV). In Sec. V, the experimental results are presented and discussed. We compare our interpretations with previous ones, and we will be able to draw conclusions from the general trends and the evolution of properties with particle size. Finally, in Sec. VI, a summary and conclusions can be found.

II. EXPERIMENTAL DETAILS

We report on ^{197}Au Mössbauer measurements on the nine materials tabulated in Table I. With the exception of the colloids, they are all molecular cluster compounds. So far these molecular compounds have not been obtainable in crystalline form, except for the Pt_{38}, so that all-atom x-ray determinations of the molecular structure have been possible only for

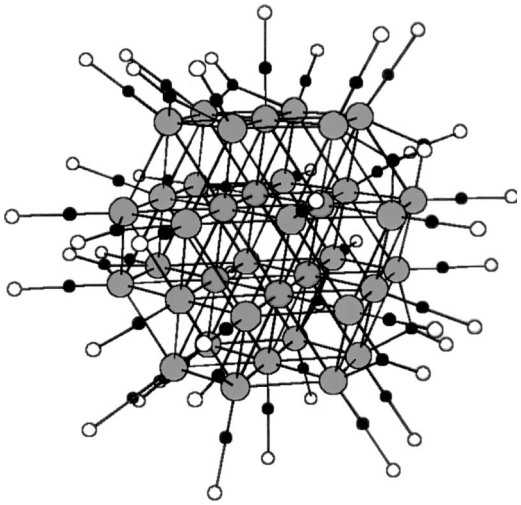

FIG. 1. Full structure of a $[Pt_{38}(CO)_{44}]^{2-}$ unit, i.e., the Pt metal core surrounded by CO ligands. The PPh_4^+ counterions are not shown. Large gray circles represent Pt atoms, small black circles are carbon, and open circles are oxygen atoms.

the latter.[7] Figure 1 shows the full structure of a $Pt_{38}(CO)_{44}$ unit, i.e., the Pt metal core surrounded by CO ligands. The PPh_4 counterions are not shown. The metal core without the ligands is shown in the left-most picture of Fig. 2. It consists of an hcp Pt_6 unit surrounded by a full shell of 32 Pt atoms in hcp packing. For the other clusters, extensive evidence based among others on EXAFS[14,16,17] and x-ray-diffraction data[3,7] has been compiled. The packing of the metal atoms in these cluster cores is fcc, and their shape is cuboctahedral, with eight triangular {111} surfaces and six square {001} surfaces (Fig. 2). We will divide the metal atoms of all particles into inner-core atoms and surface atoms. Each atom in the inner core has a cubic, 12-fold metal-atom coordination (fcc structure). For the surface atoms in the outer shell, this coordination is reduced, and some are bonded to the stabilizing ligands (cf. Figs. 1 and 3). Pt-c33 and the Au-c# series are colloidal substances, for which the numbers of metal atoms and organic ligands are only approximately known. Their sizes, and the width of the size distribution as given in Table I, are average values obtained from transmission electron micrographs. Apart from a size distribution, also a distribution in the number of ligands cannot be excluded for these large particles.

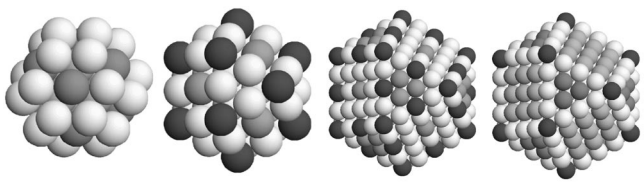

FIG. 2. Sites of the investigated molecular metal clusters. From left to right: Pt_{38} with corner and hexagon center sites. Pt2 and Au2 with corner, square face, and edge sites. Pt4phen* by ligand type, with phen* bonded (black), O_2 bonded (middle gray), and bare sites (light gray). Pt4 by metal-atom coordination, with corner, edge, square {001} face, and triangular {111} face sites.

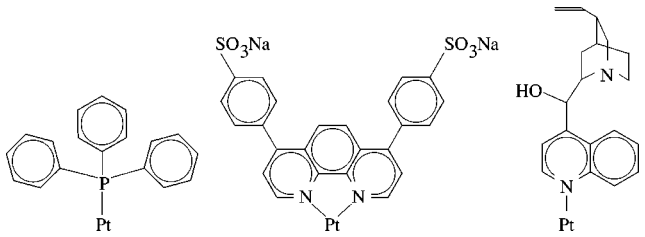

FIG. 3. Chemical formulae of some ligands. From left to right: PPh_3 (triphenylphosphine), phen* (a 1,10-phenanthroline derivative), and cinc (cinchonidine).

Emission and absorption ^{197}Au Mössbauer spectroscopy was applied to the Pt and Au particles, respectively. All samples were in the form of powders. The Au particles were measured in transmission geometry, where they were used as an absorber held at temperatures between 1.25 and 30 K. As a source, a neutron-irradiated Pt powder ($>95\%$ ^{196}Pt) was used. The resulting ^{197}Au/Pt source has a single line, with natural linewidth (0.941 mm/s)[31] and a recoil-free fraction (f factor) of 0.220 at 4.2 K, corresponding to a Debye temperature of 186 K.[32] During all measurements, the source was held at 4.2 K. The Pt particles were irradiated with thermal neutrons, and subsequently used as a source of ^{197}Au Mössbauer radiation. This was absorbed by a 37-μm-thick gold foil, held at 4.2 K. Its f factor at that temperature is 0.189, corresponding to the Debye temperature of bulk metallic gold (170 K). All spectra were recorded in the constant acceleration mode, and the velocities were calibrated using a Michelson interferometer. The emission method employed for the Pt particles has been fully described in Refs. 21 and 22. The neutron irradiation of the samples results in the reaction $^{196}\mathrm{Pt}+n\rightarrow{}^{197}\mathrm{Pt}$, followed by $^{197}\mathrm{Pt}\rightarrow{}^{197}\mathrm{Au}^{+}+\beta^{-}+\bar{\nu}_e+0.6$ MeV. The aftereffects of the β^- decay are well described in Ref. 21. For example, in the process a highly energetic electron is ejected. However, the electronic relaxation processes within the (metallic) cluster will be very short ($<10^{-15}$ s) with respect to the time scale of the Mössbauer event (10^{-9} s), so that the electronic configuration within the $(^{197}\mathrm{Au/Pt})^+$ cluster will have stabilized. The neutron-irradiation treatment was found to produce no substantial radiation damage in the Pt4phen* samples.[21]

All fits to the data are evaluations of the transmission integral,[33] so that absolute values for the recoil-free fractions (f factors) can be derived. The following values were used for the nuclear-spin $\frac{1}{2}\rightarrow\frac{3}{2}$ transition. Nuclear quadrupole moment in the ground state: $Q_{3/2}=0.594\times10^{-28}$ m^2, Mössbauer transition energy: $E_\gamma=77345$ eV, natural linewidth: $\Gamma_{nat}=0.243$ μeV (corresponding to 0.941 mm/s), and internal-conversion coefficient: $\alpha_T=4.30$, corresponding to a total effective cross section $\sigma_0=3.86\times10^{-24}$ m^2. The absorption (emission) profile is a sum over all sites, each consisting of a set of Lorentzian lines with a total relative intensity I, a quadrupole splitting QS, and a center-of-mass shift or isomer shift IS. The relative intensity I of a site is proportional to the product of the corresponding number of atoms and its f factor. This is a measure for the stiffness by which the atom is bound in the solid, and thus gives information about the phonons in the material. We note that the QS is

proportional to the electric-field gradient at the nucleus, and that the *IS* is proportional to the difference in electron density at the nucleus in the absorber compared to that in the source. All values of *QS* and *IS* in this paper are given in terms of a Doppler velocity in mm/s. This velocity v is related to a variation in the γ-ray energy E_γ by $\delta E_\gamma = E_\gamma v/c$, with c the velocity of light. The *IS* is given relative to that of a ^{197}Au impurity in a Pt foil, denoted as ^{197}Au/Pt. For the Pt particles, the *IS* values are reversed in sign, because the particles were used as a source. A value of $IS=0$ for both Au and Pt particles means that the *IS* is identical to that in bulk. Furthermore, a more positive value of the *IS* indicates a larger electron density at the probing nucleus.

III. ELECTRONIC MÖSSBAUER PARAMETERS OF METAL NANOPARTICLES

In this section, we shall clarify how size effects on the physical properties of metal nanoparticles can be probed advantageously by Mössbauer spectroscopy. A spectrum generally consists of several contributions, each arising from a different site in the particle. The local properties of each site determine the shape of the spectral contribution. Thus, provided that the local differences are large enough, the different spectral contributions can be resolved and physical information can be obtained for each site separately. More specifically, for different sites, values can be found for the *IS*, the *QS*, and the relative spectral weight *I*. The latter is a product of the abundance of the site with its (average) *f* factor. In the following, we will describe the expected size-dependent properties of our metal nanoparticles, starting with the simplest model and then making subsequent refinements. At every stage, the effects on the Mössbauer parameters will be discussed.

For a better understanding of the data, we mention here the much used *QS-IS* correlation diagram. In insulating monatomic Au complexes, the most common valence states are Au^I, when the Au atom is linearly coordinated by two ligands, and Au^{III} for a planar fourfold geometry. Other valence states or geometries are encountered only very rarely, e.g., Au^V in an octahedral sixfold geometry. Extensive experimental studies on many Au complexes have revealed clear correlations between the values of *QS* and *IS*.[25–28] All values of *IS* are found to lie between -1 and $+5$ mm/s. The *QS* in Au^I compounds depends roughly linearly on the *IS*, rising from about 4 to 11 mm/s. For Au^{III} compounds a similar linear dependence is found, but the *QS* is systematically lower than for Au^I. Figure 4 shows the so-obtained *QS-IS* correlation diagram, where the gray bands indicate the regions within which almost all literature data fall. Also a region for the rare Au^V is included. The actual data points in the diagram refer to the values resulting from various fits to the Mössbauer spectra of the materials in Table I, and will be discussed below.

We will also use the concept of a local density of states, $\rho_i^R(E)$. In its simplest form, it corresponds to the local charge density of the electronic states having a particular energy *E*. However, for the interpretation of the *QS* and *IS* it is more useful to project the electronic states onto atomlike orbitals *i* on a particular site *R*. By integrating $\rho_i^R(E)$ over *E* up to E_F, an effective number of electrons n_i in every orbital *i* can thus be found. The *QS* and *IS* are more easily related to these effective occupation numbers than to the original electronic states.

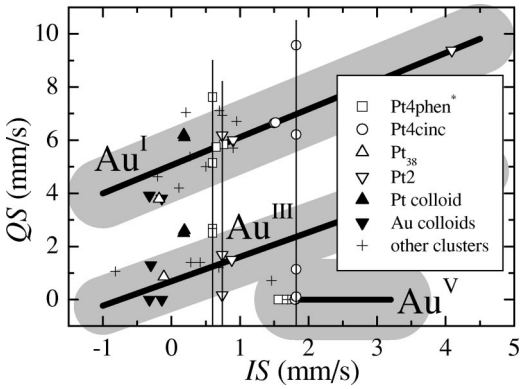

FIG. 4. Quadrupole splitting versus isomer shift diagram. The gray bands indicate the three different regions found for gold in a mono-, tri- and pentavalent state. The plus symbols show that most of the previous data (Ref. 21) (Au2 and Pt4phen) give values in these regions, with *IS* mostly between 0 and 1 mm/s. Heavy solid lines correspond to the linear relations as mentioned in the text. Vertical lines indicate the *IS* values for fits in which all surface sites were taken to have the same *IS*, but a varying *QS*.

A. Surface and quantum-size effects in free-electron-like metal nanoparticles

In the simplest model for the electronic properties of the metal nanoparticles, one may completely neglect the presence of ligands. In a first approximation, the (valence) electrons in the metal can be treated as moving in a constant potential, since the attractive potential of the nuclei is largely screened by the inner-core electrons. This model, known as the jellium model, predicts an almost uniform electron density within the metal, at positions very far from a surface. As a result of screening, the density near a surface has a damped oscillatory behavior, with a period of about half a Fermi wavelength (about 0.26 nm for Au). Calculations on an infinite plane surface of sodium[34,35] show that the amplitude of these Friedel oscillations decreases from about 10% to zero over the first 1.5 nm from the surface. Just outside the surface, there is a spillout of charge over a distance of about 0.5 nm. As the Mössbauer *IS* is sensitive to the valence electron density, similar behavior of the *IS* as a function of distance from the surface into the metal can be expected.

As the Fermi wavelength in a metal is of the order of a nanometer, strong quantum-size effects (QSE) can be expected when the particle diameter comes into the range of a few nanometers. In bulk metals, the local density of states, $\rho_i(E)$, forms a (pseudo)continuum around E_F. A single atom, on the other hand, has only discrete electronic energy levels. A nanoparticle is just in between these two extremes; $\rho_i(E)$ is discrete, as in an atom, but the distance between levels becomes smaller as the particle size, and thus the number of electrons in the particle, increases. The presence of

these quantum gaps results in dramatic effects in, e.g., the thermodynamic properties of nanoparticles, such as magnetic susceptibility, NMR, and specific heat, at temperatures lower than the average level splitting around E_F. These physical quantities crucially depend on the possibility for transitions between electronic levels around E_F. Contrastingly, the development of quantum gaps around E_F will affect the Mössbauer *IS* and *QS* much less, since these parameters depend on the *integral up to* E_F of the *local* density of states, projected onto atomic orbitals.

The quantum-size effect on the spatial variation of the electron density inside the particles can again be assessed qualitatively on the basis of jellium-model calculations for simple metal clusters. When the particles are approximated by spheres, the electrons are organized into atomlike orbitals, resulting in an electronic shell structure.[36] Proof for the presence of such a shell structure in real clusters has been found for alkali-metal clusters produced in beams.[37,38] As in every atomlike system, the electron density depends strongly on the distance from the center of the spherical potential. Detailed calculations for the spherical jellium model, evaluated at zero temperature,[39] show that the electron-density fluctuations can be as large as 50% of the average density for Na particles containing up to 58 atoms. For increasingly larger particles, the oscillations evidently smear out, and the electron-density variation approaches more and more the (Friedel oscillation) profile, appropriate for an infinite plane metal surface. These considerations show that the QSE may lead to a spatial variation of the *IS* throughout a nanoparticle, in particular since the *IS* is very sensitive to the $6s$-electron density.

Thus we have identified two possible mechanisms by which the Mössbauer *IS* can vary as a function of distance to the surface. For small particles (with a radius up to about 1.5 nm), the (Friedel) oscillations due to surface screening will be appreciable over the whole particle, and it will be difficult to distinguish them from oscillations due to the QSE. For the larger particles, the latter will gradually disappear, restricting the fluctuations to the Friedel oscillations in the outermost layers.

B. Local density-of-states approach (tight binding)

Next, we have to take into account that our nanoparticles consist of the $5d$-transition metals Au and Pt, instead of a free-electron-like metal. Full molecular-orbital calculations on one-shell Pt_{13} clusters (and other small particles)[40] show that the shapes of the cluster orbitals around E_F resemble those of localized $5d$ orbitals, which are deformed at the particle surface, following the local coordination. From such calculations one could in principle also derive quantitative values for the Mössbauer parameters (*IS* and *QS*) using a local density-of-states (LDOS) approach. However, since the computational effort is very large for Au and Pt particles with more than say 50 atoms, we cannot resort to a full calculation of the molecular orbitals here. Instead, we will use the local density of states with more qualitative arguments to gain some insight into the Mössbauer parameters.

The projection of the total wave functions onto definite atomic orbits allows one to treat $5d$, $6s$, and $6p$ electrons separately. The relatively high-energetic $6p$ electrons only become relevant when they are covalently mixed with ligand orbitals or affected by crystal-field splitting. Therefore, we will neglect them for the moment. In gold and platinum metal, the $6s$ electrons are highly delocalized, and can be treated as nearly free. The results of the previous subsection may be applicable to them, assuming a separation into $6s$- and $5d$-electron contributions as a reasonable approximation for our purpose.

The $5d$ electrons are, even in the metallic state, to a large extent localized, so a tight-binding model can be used to evaluate the changes produced at the surface. It is useful to recall that the reduced metal-atom coordination at the surface narrows the LDOS at the surface, $\rho_{5d}^{surf}(E)$. Layer-resolved (slab) calculations on $\rho_i^j(E)$ (as a function of atomic layer j, counted from the surface), in a tight-binding solid, show as a very general result that the LDOS ''heals'' back to the bulk structure in at most two or three atomic planes.[41] Analogous results are found in layer-resolved density-functional calculations on large Au clusters.[29,42] The narrowing of the LDOS at the surface has been verified in several experimental studies.[43,44] A similar healing model has also been used to explain NMR data on Pt nanoparticles in catalysts,[45,46] and also specifically in an NMR study on the same Pt4phen* clusters as investigated in this paper.[19] There, the $5d$ LDOS at E_F was assumed to decrease near the surface over a healing length of about 0.6 nm,[19] which is much more than a single atomic layer. The narrowing of the $5d$ band results in an increase of n_{5d}^{surf} at surface atoms, for more than half-filled $5d$ bands (like in Pt and Au). This results in an upward shift of all levels at the surface, effectively increasing n_{5d}^{surf} at the cost of n_{6s}^{surf}. The redistribution of electrons was shown to happen mainly at the surface layer.[47] Calculations on these surface level shifts[48] S, in cuboctahedral Au2 clusters, give values of $S=1.09$, 0.87, and 0.63 eV for, respectively, the corner, edge, and face atoms.[29] The width of the $6s$ band is about 15 eV. We can thus estimate Δn_{6s}^{surf} due to the surface level shift, by assuming a constant LDOS over the whole $6s$ band. This band can obviously accommodate two electrons, so $\Delta n_{6s}^{surf} \approx 2S/15$, leading to $\Delta IS \approx -1.2$, -0.9, and -0.7 mm/s, respectively, since a change of one $6s$ electron changes the *IS* roughly by $+8.0$ mm/s.[49] We can conclude that possible variations in the *IS* over the surface (within 0.5 mm/s) will be much smaller than those in insulating monatomic Au complexes (over about 5 mm/s).

Another important effect of the surface is the reduced local symmetry, imposed by the decrease in the metal-atom coordination, varying from site to site over the surface. In crystal-field theory, the order and occupation of the $5d_m$ levels (with a different z component of the orbital momentum, indicated by the quantum number m) depend on this symmetry. Similarly, the $6p_{x,y,z}$ levels will be affected, and may become partially populated, which can have large consequences for the value of *QS*. Also the periodic potential of the bulk is cut off, which allows for the formation at the surface of new exponentially decaying solutions to the

Schrödinger equation. The energy of such a surface state lies in a bulk band gap. The surface density of states is increased in the gap, at the cost of density at nearby band edges.[50] Although $\rho_i^{surf}(E)$ can thus change significantly at the surface, the influence of localized surface states on n_{6s}^{surf} is probably negligible, since E_F is not close to the $6s$-band edges. Still, the proximity of E_F to the top of the $5d$ band may cause changes in $n_{5d_m}^{surf}$, due to the formation of such surface states.

Summarizing, we have argued in the above that variations in n_{6s}^R, inside the metal particles, will be mainly caused by Friedel oscillations and QSE. On the other hand, $n_{5d_m}^{surf}$ and $n_{6p_n}^{surf}$ are mainly influenced by the local symmetry of the surface sites. $n_{5d_m}^{surf}$ can be further affected by $5d$-band narrowing, surface level shifts, and possibly the formation of surface states, whereas n_{6s}^{surf} will be roughly constant. Since the number of nearest neighbors is different for the various surface sites in our cuboctahedral clusters, the degree of $5d$-band narrowing will also vary. Thus, we may expect a correlation of $n_{5d_m}^{surf}$ and $n_{6p_n}^{surf}$ (and so of the QS) with the geometry of the site on the cluster surface. These surface effects may cause changes in $\rho_i^R(E)$ deeper into the bulk as well, e.g., in the layer directly below the surface layer.

C. The effects of ligation

In ligated molecular metal clusters, many of the surface atoms have chemical bonds to the ligands, or are influenced by (possibly charged) adsorbed atoms and small molecules, as, e.g., $O_2^{-\delta}$. This has consequences, not only directly for these surface atoms, but also for the structural and electronic properties of the cluster as a whole. As regards structural aspects, it is important to recall here that the structural stability of ligated metal clusters is to a large extent determined by the ligand shells.[1,2] The steric repulsion between voluminous ligands can cause an expansion of the volume of the particle metal core.[42] On the other hand, the surface tension becomes an important term in the free energy of a small particle, because of the large surface-to-volume ratio. In general, this is expected to cause a volume contraction in freely suspended bare metal clusters.[29,42,51,52] A direct result of a reduced particle volume is an increased average electron density, and thus an increased average value for IS. For ligated cluster compounds, it is of interest, in this respect, to note that even for relatively small clusters, the metal-metal distances inside the cores are quite close to bulk values. E.g., in Pt_{38} (Ref. 7) and Pt4phen*,[17] most of the bond lengths are within 1% of the bulk value.

Regarding the electronic properties, the presence of (charged) adsorbed molecules and atoms has to be considered in addition to the effects of the surface itself, as described in the previous subsections. The monopole and dipole moments of the adsorbates will result, as before, in changes of $\rho_{6s,6p,5d}(E)$ at the surface. However, since the Thomas-Fermi screening length in Au is of the order of half an interatomic distance, any surface effect is screened very effectively by the delocalized $6s$ electrons, resulting in a very fast recovery of $\rho_{6s,6p,5d}(E)$ deeper into the particle.

Chemical bonds may have additional effects. One comes from charge transfer to the metal particle, resulting in a slight change of the Fermi level. The resulting changes in n_{6s}, n_{6p_n}, and n_{5d_m} in the inner core of the particle probably decrease with increasing particle size, since the charge change is delocalized over the whole particle. Another effect due to the mixing of ligand orbitals with surface metal-atom $5d$, $6s$, and $6p$ orbitals could be that the occupation of these surface metal-atom orbitals and their contribution to the values of QS and IS might become comparable to those found in insulating monatomic Au complexes. This could happen when the ligation of the surface atom results in a charge localization. As long as there are metallic bonds between the surface atoms and the rest of the particle, these atoms will tend to keep their charge equal to that in the inner core, prohibiting the formation of definite valence states. If, however, the metallic character of these bonds is lost, charge may accumulate on the individual surface atoms and their QS and IS values could become reminiscent of Au^I or Au^{III}. The correlation between QS and IS would then depend on the symmetry imposed by the ligands in combination with their image potentials. That mixing of ligand orbitals with those of the surface metal atoms can indeed have large consequences on the effective number of electrons in the different orbitals is confirmed by calculations and experiments on carbonylated Ni clusters.[13] There, the CO σ orbitals repel the $4s$ orbitals of surface atoms, which causes an increase of n_{3d} at the cost of n_{4s}. Ultimately, the $3d$ band was predicted to become completely filled at the surface, which explains in fact the experimentally observed quenching of the magnetic moments on the Ni atoms, at the surface of Ni carbonyl clusters.[53]

It is noteworthy that in very small ligated clusters, such as, e.g., Au_3Fe,[54] $AuRu_2$,[55] and Au_2Ru_3,[55] low values of IS were measured (0.7–2.1 mm/s), which was attributed to a relatively low population of Au $6s$ orbitals, supposedly caused by a donation of these $6s$ electrons to a cluster orbital which is delocalized over all metal atoms. Also in ligated Pt_3Au and Pt_3Au_2 clusters, such a correlation between the Mössbauer parameters and the degree of electron delocalization was found.[56] There, it was also found that the Mössbauer parameters do not depend much on changes in the bridging (PPh_3-like) ligands between the Pt atoms. Thus, even in clusters containing only four metal atoms, electronic delocalization was found, and correlates with low values (below 2 mm/s) of the IS.

We can thus make a distinction between a ''metallic'' and a ''nonmetallic'' ligated surface layer. *We define a "metallic" surface layer as one that is part of the total volume over which the electrons are delocalized.* In that case, charge can be freely interchanged between surface metal atoms and the inner core, and the surface may keep its charge per atom close to that in the rest of the particle. Nonetheless, due to effects like the QSE described above, the LDOS at the surface can still differ from that in the inside of the particle. In the opposite case of charge localization at the surface metal-

atom orbitals, individual surface atoms may develop local valence states, and the values of *QS* and *IS* of these surface sites would increase, and correlate with the type of ligand coordination found in monatomic Au complexes. For the ''metallic'' surface layer, however, the *QS* may still be correlated with the local metal-atom coordination of the surface site, whereas the *IS* should be roughly constant over the surface, at a low value, probably below about 2 mm/s. We will investigate the applicability of both scenarios in Sec. V.

IV. VIBRATIONAL MÖSSBAUER PARAMETERS: SIZE EFFECTS ON THE PHONON MODES

The phonon modes in small particles are substantially different from those in bulk. Since Mössbauer-effect spectroscopy is a local probe for the atomic vibrations, this has large consequences for the *f* factors (recoil-free fractions) of the various atoms in the particle. Due to the size effect (small number of atoms), the number of available phonon modes is relatively small, so the concept of a continuous phonon density of states, as in the bulk, can no longer be used. Instead, other models like the elastic continuum approximation[57] or a central force model[20] allow the calculation of the phonon modes inside the particle, and lead to a discrete phonon density of states. This discreteness results in the formation of a low-frequency cutoff in the phonon spectrum, similar to the gap around E_F in the electronic density of states as a result of the QSE. We will employ a refinement of the central force model already used by Smit *et al.*[20] to calculate the *f* factors of each individual atom in a cluster. We describe here the most important aspects of this model.

The emission (absorption) of a Mössbauer photon results in a transfer of the momentum of the photon to the lattice. A fraction f^{intra} of all emissions (absorptions) results in a recoil of the particle as a whole, whereas otherwise the emitting (absorbing) atom recoils, and creates a vibration in the particle, a so-called intraparticle phonon. This fraction f^{intra} can be obtained from the central force model, as described by Smit *et al.*,[20] which depends on a matrix *V* of second derivatives of the central potential in which each atom moves. The matrix elements have the dimensions of a force constant *C*, and describe the interaction strength between two atoms.

If the momentum is transferred to the particle as a whole, this recoil momentum is subsequently transferred either to a phonon in the two-component medium of ligands plus metal cores (interparticle vibrations in the matrix), or to the whole sample. The two-component matrix can be approximated by an effective Debye solid,[21] with Debye temperature θ_D^{inter}, so the usual Debye formula for the recoil-free fraction can be applied. [See Ref. 58, p. 61, Eq. (3.84).] The fraction of all particle recoils that results in a transfer of momentum to the whole sample can thus be obtained. This fraction is called the interparticle *f* factor, f^{inter}. As usual for a Mössbauer event, the associated energy loss for the recoil of a macroscopic sample, as a whole, is much less than the natural Mössbauer linewidth, and thus a resonant emission (absorption) occurs. The analysis of *f* factors depends further on the assumption that the net resonant fraction of photon emissions (absorptions) equals the fraction of photon emissions (absorptions) which result in a recoil of the particle as a whole, times the fraction of all particle recoils resulting in a resonant emission (absorption):

$$f_i = f^{inter}(\theta_D^{inter}) f_i^{intra}(C).$$

The validity of this approximation can be expressed by the statement that the inter- and intraparticle vibrations are completely decoupled: $\langle|\mathbf{u}|^2\rangle_{tot} = \langle|\mathbf{u}|^2\rangle_{inter} + \langle|\mathbf{u}|^2\rangle_{intra}$, where $\langle|\mathbf{u}|^2\rangle$ is the mean-square displacement of the atom. Another way of saying this is that the interparticle phonons in the soft matrix do not interact with the intraparticle phonons, except when the latter have a zero-wave vector, in which case the interaction represents the recoil of the particle as a whole, which can result in the creation of an interparticle phonon.[59]

Smit *et al.*[20] considered homonuclear clusters, with only nearest-neighbor interactions, in their model. Since all atoms are identical, they needed the value of only one force constant *C* to find f_i^{intra} for all atoms *i* in the cluster. For Au particles, this presents no problem, so we will take exactly the same model with $C_{\text{Au-Au}}$ as the force constant. For the Pt particles, however, due to the application of the emission technique, the probing atom is not a Pt atom, but an Au atom in a Pt matrix (cf. Sec. II). The force constant describing the interaction between this Au atom and its Pt neighbors will be different from that between the Pt atoms themselves. Thus we will introduce two force constants $C_{\text{Au-Pt}}$ and $C_{\text{Pt-Pt}}$ into the matrix *V*, from which again all f_i^{intra} are calculated. This involves a different matrix *V* for every (inequivalent) position of the Au atom in the Pt particle, since changing the location of the Au atom affects all phonon modes of the particle. In any case, f_i^{intra} varies from atom to atom in the particle, and depends strongly on the number of nearest neighbors. A surface atom is less tightly bound to the crystal than an atom in the inner core, and its *f* factor will be lower. (See also Table II.)

For a reliable and unbiased analysis, it is important to obtain, as a reference, bulk values for $C_{\text{Au-Au}}$, $C_{\text{Au-Pt}}$, and $C_{\text{Pt-Pt}}$ from other experimental quantities that may be measured in bulk solids. These values can be used either to compare with experimental values, as obtained from fitting the Mössbauer spectra, or as fixed parameters in modeling our nanoparticles. In the latter approach, the only remaining free fitting parameter to describe all *f* factors is θ_D^{inter}, giving information about the stiffness of the matrix (ligands plus metal particles).

In order to obtain values of the force constants for the bulk, which can reliably be used for the cluster *f*-factor analysis, it is best to use exactly the same central force model to calculate a bulk *f* factor, and adjust the force constant so that this bulk value is equal to that experimentally found. Denoting the zero-temperature limit of *f* as f_0, in this model[20] $-\ln f_0 \propto E_R \Sigma_s (A_s^2/\omega_s)$. Here ω_s is the frequency of vibration mode *s*, which is in general proportional to $\sqrt{C/M}$. A_s is a normalized vibration amplitude of mode *s*, and does not depend on the atomic mass *M* or on *C*. E_R is the recoil energy of an atom, which is inversely proportional to its mass *M*. Thus $-\ln f_0 \propto 1/\sqrt{MC}$, so that $D \equiv -\sqrt{MC}\ln f_0$ is a

TABLE II. Calculated intracluster f factors for all crystallographically different atoms in Pt4, Pt2, and Pt_{38} clusters at $T=4.2$ K, using the central force model with $C_{\text{Pt-Pt}}=45.3$ N/m, and $C_{\text{Au-Pt}}=27.4$ N/m. The numbers in the first column refer to the shell number within the cluster, and the abbreviations in parentheses are used in the text for the various surface sites. n is the number of atoms occupying each site, and nn is the number of nearest neighbors. $I_s \equiv 100 N_s f_s^{intra}/\Sigma_i N_i f_i^{intra}$ is the relative intensity of each site in the Mössbauer emission profile of the Pt particles.

Pt4	n	nn	f^{intra}	I (%)
0	1	12	0.2303	0.42
1	12	12	0.2300	5.03
2 corner	12	12	0.2279	4.99
2 edge	24	12	0.2287	10.01
2 square	6	12	0.2291	2.51
3 corner	12	12	0.2126	4.65
3 edge	48	12	0.2189	19.17
3 square	24	12	0.2219	9.72
3 triangle	8	12	0.2226	3.25
4 (c) corner	12	5	0.0785	1.72
4 (r2) edge 2	48	7	0.1247	10.92
4 (r1) edge middle	24	7	0.1305	5.71
4 (s3) square corner	24	8	0.1486	6.51
4 (s2) square edge	24	8	0.1515	6.63
4 (s1) square middle	6	8	0.1538	1.68
4 (t) triangle	24	9	0.1616	7.08
Pt2				
0	1	12	0.2428	2.82
1	12	12	0.2363	32.96
2 (c) corner	12	5	0.0938	13.08
2 (e) edge	24	7	0.1420	39.61
2 (s) square	6	8	0.1654	11.53
Pt_{38}				
Core	6	12	0.2439	23.23
(c) corner	24	6	0.1373	52.32
(h) hexagonal center	8	9	0.1925	24.45

(positive) constant depending on the crystal structure and the γ-ray wave vector only. We calculated D for a central atom surrounded by a varying number N of full shells of atoms, retaining the fcc structure. In Fig. 5, we have plotted D as a function of $1/N$. Extrapolating to $1/N \rightarrow 0$ (an infinite number of shells), we find for the bulk $D^{bulk}=4.75(6)\times 10^{-12}$ kg/s, which should be a universal number for all monatomic fcc materials. The value $f_0^{bulk-\text{Au}}=0.190$ is observed from extrapolation to $T=0$ K from the experimental value for gold at 4.2 K (with the usual Debye formula[58]), and leads with D^{bulk} to $C_{\text{Au-Au}}^{bulk}=25.0(6)$ N/m.

In order to obtain a value for $C_{\text{Pt-Pt}}^{bulk}$, we utilize the general relation between the force constant in a crystal and the Debye temperature $C_{\text{fcc}}=\alpha M \theta_D^2$. Here α depends only on the lattice structure. Already in 1911, Einstein pointed to such a proportionality,[60] and although different numerical predictions have been made for α, the relation itself has never been contested.[61] From the above-derived value for $C_{\text{Au-Au}}^{bulk}$, obtained from the experimental f factor of gold, and taking the Debye temperature of gold $\theta_{\text{Au}}=170$ K, as obtained from specific-heat measurements (see Ref. 62, p. 461), we derive $\alpha=2.64(8)\times 10^{21}$ $\text{s}^{-2}\text{K}^{-2}$. This, together with $\theta_{\text{Pt}}=230$ K (see Ref. 62, p. 461), can be used to find a value for $C_{\text{Pt-Pt}}^{bulk}=\alpha M_{\text{Pt}} \theta_{\text{Pt}}^2$, which leads to $C_{\text{Pt-Pt}}^{bulk}=45.3\pm 1.1$ N/m. We note that a numerical evaluation of α on the basis of the central force model and the Debye model yields $\alpha=3.9\times 10^{21}$ $\text{s}^{-2}\text{K}^{-2}$, which is in reasonable agreement with the above-mentioned empirical result.[63]

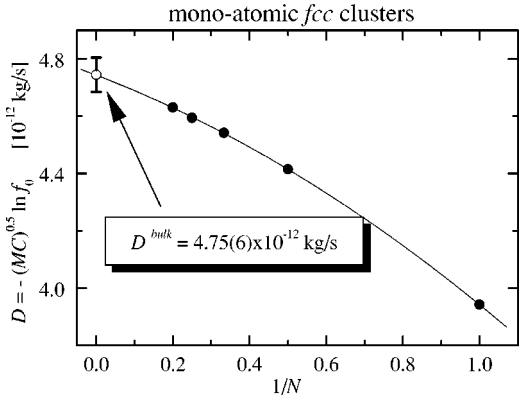

FIG. 5. D (proportional to the logarithm of the f factor at zero temperature, see text) as a function of the inverse number of shells, surrounding a central atom. The open symbol with error bars represents the extrapolation to zero, corresponding to a bulk fcc lattice. See the text for further details.

We also need a value for the force constant of an Au-Pt bond $C_{\text{Au-Pt}}^{bulk}$. We expect $C_{\text{Au-Pt}}^{bulk}$ to be much lower than $C_{\text{Pt-Pt}}^{bulk}$ on the basis of the low Debye temperature for bulk ^{197}Au/Pt, which equals 186 K,[32] as derived from a calibration of the f factor of a ^{197}Au/Pt source at 4.2 K. This is much lower than θ_{Pt}, almost as low as θ_{Au}.

We use a similar procedure as above for pure gold to obtain a value for $C_{\text{Au-Pt}}^{bulk}$. Assuming $C_{\text{Pt-Pt}}=45.3$ N/m, as derived above, and varying the values for $C_{\text{Au-Pt}}$, the f factor is calculated of a single central Au atom surrounded by an increasing number N of full shells of Pt. In Fig. 6 we plotted $-\ln f_0$ as a function of $1/N$. $C_{\text{Au-Pt}}$ is adjusted such that the extrapolation to $1/N \rightarrow 0$ (the bulk ^{197}Au/Pt limit) is consistent with $-\ln f_0=1.510$, which is derived from the experimental value $f(T=4.2\ \text{K})=0.220$ using the Debye model. The result is $C_{\text{Au-Pt}}^{bulk}=27.4\pm 1.2$ N/m.

It is interesting to note that $-\ln f$ decreases (f increases) with decreasing particle size (cf. Figs. 5 and 6). This can be understood in terms of the quantum-size effect on the phonons, which should lead to a low-frequency cutoff in the phonon density of states (see, e.g., Ref. 64). The average size of the low-frequency cutoff should scale with the inverse volume of the particle. In crude terms, one could say that phonon modes with a wavelength larger than the particle diameter do not fit in. From the factor $1/\omega_s$ in the formula for f^{intra},[20] $-\ln f^{intra} \propto E_R \Sigma_s (A_s^2/\omega_s)$, it can be easily seen that the largest contribution to this sum comes from the low-

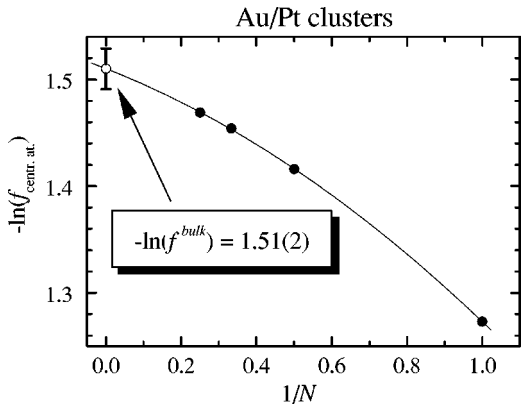

FIG. 6. The logarithm of the f factor at $T=0$ K, as a function of the inverse number of Pt shells, surrounding a central Au atom (solid circles). The open circle with error bars is the extrapolation of the solid symbols to zero, corresponding to bulk Au/Pt. Using $C_{\text{Pt-Pt}}=45.3$ N/m, we adjusted $C_{\text{Au-Pt}}$ in the calculation of the solid symbols so that the extrapolated value coincides with the experimental value of 1.51 (derived from the experimentally obtained f factor of 0.221). Thus, we found $C_{\text{Au-Pt}}=27.4\pm1.2$ N/m.

frequency phonon modes. The low-frequency cutoff in small particles results thus in systematically higher values of ω_s, leading to an increase of f^{intra}.

In the next section, we will present the experimental results of the Mössbauer investigations. We will use f factors calculated from the above-derived bulk force constants. In Table II, we have collected the result for f^{intra} of all crystallographically different atoms in the investigated molecular Pt clusters. In the actual analysis, many of these atoms are taken together, and treated as a single site, with the same IS and QS. The relative intensity I is then simply the sum of all separate values I_s for all atoms s in the site.

V. EXPERIMENTAL RESULTS

After the above preparatory steps, we now have a sufficient basis to present and discuss the experimental Mössbauer spectra for the particles tabulated in Table I. We start with the ^{197}Au Mössbauer spectra of the Pt4 nanoparticles, followed by the successively larger Pt and Au colloids. Finally, we discuss the spectra of the Au2tpp, Pt2, and Pt_{38} particles in light of the results obtained from the large particles. As part of the procedure, we will reanalyze three ^{197}Au Mössbauer spectra which were previously recorded and published by Mulder *et al.*[21] (on Pt4phen* and Au2tpp), and by van de Straat *et al.*[23] (on Pt_{38}). We remind here that ^{197}Au Mössbauer measurements on Pt_x particles are actually done on $(Pt_{x-1}Au)^+$, due to the conversion of one Pt atom into Au by the neutron irradiation. Since the differences between the electronic configurations of Au and Pt are not very large, we will use the $(Pt_{x-1}Au)^+$ particles as models for the original Pt_x particles.

Mulder *et al.*[21,22] analyzed the f factors within the central force model using a single intracluster force constant, the values of which were found to deviate strongly from those derived from bulk properties. This discrepancy was attributed to a lattice softening in the nanoparticles.[21,65] Although the force constants appeared to agree with specific-heat data on the Pt4phen* cluster,[65] it was later pointed out by Volokitin that the ligands can contribute strongly to the specific heat.[66] He showed that for ligand-stabilized Pd particles, after subtracting the contribution of the ligands, the specific heat related to the intraparticle vibrations could be explained well with the bulk speed of sound, and thus without any lattice softening. In Au2tpp particles, a change of lattice stiffness was observed, with a simultaneous lattice contraction.[14] In Pt_{38} and Pt4phen*, most of the interatomic distances deviate at most by 1% from the bulk value, as observed from x-ray[7] and EXAFS (Ref. 17) studies, respectively. Therefore, we will assume that the Pt nanoparticles are, like the Pd clusters, not subject to any lattice softening. Instead, as described in the previous section, we shall put as our basis that the central force model for the f factors applied to the Mössbauer data in Pt particles needs two force constants, and we will use the values as derived above from bulk parameters ($C_{\text{Au-Pt}}=27.4$ N/m and $C_{\text{Pt-Pt}}=45.3$ N/m) to calculate the relative intensity I for each site separately (cf. Table II). We will show below that this leads to quite satisfactory fits to the experimental data.

When comparing the measurements of the larger particles (see Figs. 7–10) with the data on the Au2 series (see Fig. 11 below), one can see immediately that the structure in the former spectra is less pronounced. Therefore, to model these spectra, not all parameters for all sites can be left free in the fits to the data. We have to make some physically plausible assumptions, in order to fix or to correlate some parameters. First, since we will assume that the refined central force model (with two force constants) can be applied, all relative intensities I can be fixed. Second, based on the considerations of Sec. III C, we will compare the two scenarios in which either the various surface metal atoms are in a definite valence state, corresponding to a ''nonmetallic'' particle surface, or that they all have the same IS value, corresponding to a ''metallic'' surface layer. In a ''nonmetallic'' surface layer, the atoms will have effective charges, with IS and QS values similar to those in monatomic Au complexes, due to the ligands attached to these surface atoms. In this scenario, we will use the IS as a free parameter, restricted to the range of from -1.0 to $+4.5$ mm/s for Au^I and Au^{III} and from $+1.5$ and $+3.5$ mm/s for Au^V. Furthermore we can calculate the QS from the IS, using the relations $QS^I=5.05+1.06\times IS$ for Au^I, $QS^{III}=0.68+0.92\times IS$ for Au^{III}, and $QS^V=0$ for Au^V, which correspond to the solid lines in Fig. 4 and are representative of the observed empirical relationships between IS and QS. Which ligand leads to which valence state of the corresponding atom remains to be determined by fitting the experimental data, assuming various combinations. The second assumption—having a ''metallic'' surface layer—corresponds to a model with a single IS value as a free parameter for the whole surface. The QS is then left free and is assumed to correlate with the local metal-atom coordination of the probing Au atom. Finally, for all the atoms in the inner core of the particles we shall put $QS=0$, but allow the electron density (and thus the IS) to vary for different successive shells of atoms within the inner core. Since we

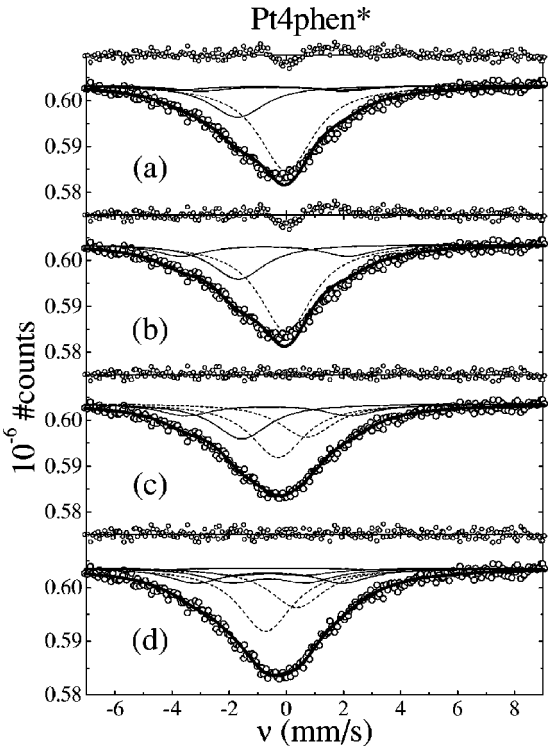

FIG. 7. Four different fits to the same data of Pt4phen* taken at $T=1.8$ K. Large open circles are the data points. The heavy solid line is the model, and the other lines are guides to the eye, representing the contribution of each different site. Dashed lines are core sites, the others surface sites. Small circles on the top axes are the differences between data and model. (a) Parameters taken from Ref. 18. (b) Single core site, nonmetallic surface. (c) Two core sites, nonmetallic surface. (d) Two core sites, metallic surface. See the text for more detailed information.

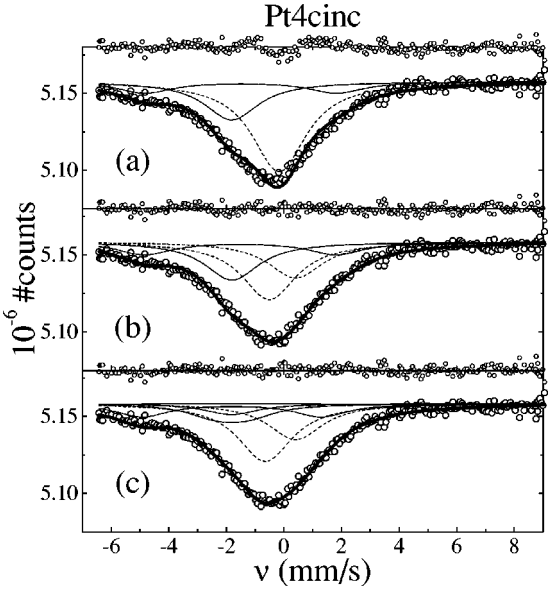

FIG. 8. Three different fits to the same data taken on Pt4cinc at $T=4.2$ K. Symbols as in Fig. 7. (a) Single core site, nonmetallic surface, $\theta_D^{inter}=7.3$ K. (b) Two core sites, nonmetallic surface, $\theta_D^{inter}=7.9$ K. (c) Two core sites, metallic surface, $\theta_D^{inter}=8.0$ K.

assume an uncontracted lattice in the Pt particles, we don't have to correct *IS* for any volume change.

A. The four-shell $Pt_{309}phen^*_{36}O_{30\pm10}$ and $Pt_{309}cinc_{102}(HAc)_{369}$ clusters

The results of a detailed reanalysis of the previously published Pt4phen* Mössbauer spectra are presented first. Figure 7(a) shows the spectra recorded by Mulder *et al.*,[21,22] together with their analysis. Inside the spectrum several lines are drawn as guides to the eye, representing contributions from different sites. In their analysis, Mulder *et al.* used a single force constant, and the surface sites were correlated with the attached ligands. Both the *QS* and *IS* for each site were taken as free fit parameters. On the basis of the molecular structure and chemical composition, they assumed the following ligand coordination: 36 phen* ligands on each corner and on each edge, and 14 O_2 molecules on the center of each square and triangle. Accordingly, the surface was divided over three sites (for the abbreviation of sites, see Table II): 36 atoms connected to phen* (c,e_1), 30 to O_2 (s_1,t), and 96 bare atoms (e_2,s_2,s_3).

Mulder *et al.*[21,22] found the resulting *QS-IS* pairs for the surface sites to lie in the region of Au^V for the unligated, bare site, and in that of Au^I for the ligated sites with a slightly different position in the *QS-IS* diagram for phen* and O_2 bonded sites (see Table III, and Fig. 4). They could not give a satisfactory explanation for the presence of a site with *QS-IS* in the region for Au^V. All 147 atoms in the three core shells were taken to be equivalent, implying a single value for the electron density throughout the core. *IS* for this single core site was found to be equal to the bulk ^{197}Au/Pt value. From this it was concluded that the electron density in the inner core is indistinguishable from that in the bulk metal, so that the influence of surface ligation is already completely screened by the electrons in the outer shell of surface atoms. From a fit of the temperature dependence of the *f* factors between 1.8 and 40 K, $\theta_D^{inter}=17$ K was found, and $C=26$ N/m. These values were in reasonable apparent agreement with an earlier analysis of specific-heat data on this compound by Baak *et al.*[11,65,67] ($\theta_D^{inter}=15$ K and $C=20$ N/m). The deviation of the fit from the data near -1 mm/s, as clearly seen in the difference plot of Fig. 7(a), was neglected at the time.

Based on the considerations in Sec. III, we now present improved fits to the same data. As explained above, there is experimental evidence that the intraparticle vibrations of Pt4phen* can be modeled using bulk parameters, so we now use the relative intensity *I* as derived from $C_{\text{Au-Pt}}=27.4$ N/m and $C_{\text{Pt-Pt}}=45.3$ N/m (the values for bulk ^{197}Au/Pt, cf. Sec. IV and Table II), and $\theta_D^{inter}=15$ K, as found from the specific-heat data by Baak *et al.*[65] The thus calculated temperature dependence of the total *f* factors fits the experimental data just as well as before[21] (not shown).

In Fig. 7(b), a fit is plotted, where we took $IS=0$ mm/s for the whole inner core, and a ''nonmetallic'' surface layer. The number of free parameters was reduced by using the linear relations between the *QS* and *IS*. We took the 66 atoms bonded to phen* or O_2 together in a single Au^I site,

TABLE III. Parameters of the fits in Fig. 7. Fixed parameters are indicated by bold faced values. The reduced χ^2_{red} values are defined as $[\Sigma_i(data_i-model_i)^2/model_i]/N$, with N the number of degrees of freedom of the fit, equal to the number of data points minus the number of free fitting parameters. A value of $\chi^2_{red}=1$ is considered a good model for the data. The relative intensity I of each site was fixed to the calculated values (cf. Table II). Values of *IS* and *QS* are given in mm/s. *IS* is with respect to ^{197}Au/Pt, and reversed in sign (see text). In (a) and (b) a single core site was used, whereas in (c) and (d) this site has been separated in two contributions. In (b) and (c) the surface sites are assigned according to the attached ligands, and *QS* was calculated from *IS* depending on the indicated valency. In (d) the surface sites are assigned according to the local metal-atom coordination (cf. Fig. 2 and Table II), and only a single *IS* value was used to fit all surface sites.

Pt4phen* (a), $\chi^2_{red}=1.56$	*IS*	*QS*	*I* (%)
Core 0–3	0.00		**60**
Phen* (c,e_1)	0.9	5.7	**7**
O_2 (s_1,t)	0.5	5.0	**9**
Bare (e_2,s_2,s_3)	1.7	0.0	**24**
Pt4phen* (b), $\chi^2_{red}=1.62$			
Core 0–3	**0.00**		**60**
Ligated (c,e_1,s_1,t)	0.8	Au^I	**16**
Bare (e_2,s_2,s_3)	1.7	Au^V	**24**
Pt4phen* (c), $\chi^2_{red}=0.97$			
Core 0–2	−0.71		**23**
Core 3	0.29		**37**
Ligated (c,e_1,s_1,t)	0.7	Au^I	**16**
Bare (e_2,s_2,s_3)	1.6	Au^V	**24**
Pt4phen* (d), $\chi^2_{red}=0.99$			
Core 0–2	−0.37		**23**
Core 3	0.73		**37**
Corner (c)	0.6	7.6	**2**
Edge (e_1,e_2)	0.6	5.1	**16**
Square (s_1,s_2,s_3)	0.6	2.7	**15**
Triangle (t)	0.6	2.5	**7**

and all 96 bare atoms in an Au^V site, as suggested by the work of Mulder *et al.*[21,22] [fit shown in Fig. 7(a)]. A fit was made with only two free parameters, namely, the *IS* for bare and bonded surface sites, from which the *QS* was calculated. As can be seen, the fit in Fig. 7(b) is very similar to that in Fig. 7(a). Thus, we can indeed explain the *f* factors in the Pt4phen* particles without having to assume an artificial lattice softening, in agreement with the reanalysis of the specific-heat data. Furthermore, limiting the *QS*-*IS* pairs to the heavy solid lines of Fig. 4 appears to be a valid way to reduce the number of free parameters.

Still, the fit on the basis of one single line, with natural linewidth and $IS=0$ for the inner core of the particle, deviates substantially from the data around the inner-core contribution. To improve the fit, we can either allow for $QS\neq 0$, or introduce more than one site for the core. A nonzero *QS* in the core is very unlikely, since the atomic packing in the core is cubic, as in the bulk. On the other hand, as explained in the above, the *IS* may vary throughout the core due to the (combination of) QSE and surface screening effects. With this in mind, we attempt another fit, in which we divide the inner core into two contributions, namely, the 55 atoms in the innermost two shells and the 92 atoms in the third shell. The *IS* value of both contributions is left free, whereas the *QS* is assumed to be zero. With these changes we obtain the fit plotted in Fig. 7(c), with parameters given in Table III. As can be clearly seen, the difference plots no longer show any deviations. It is important to stress that *a similarly good fit can only be obtained by splitting the core into two contributions with different IS*. We interpret this as evidence for a varying electron density throughout the core of the Pt4 particles, caused either by surface screening, or by the QSE, or by a combination of both. To the best of our knowledge, this is the first time that such experimental evidence has been obtained from Mössbauer spectroscopy. We note that in the other microscopic technique mentioned above, namely, the measurement of the NMR line shape[19,46] of this compound, the variation of the LDOS *around* E_F is involved. In contrast, from the Mössbauer spectra we here find experimental evidence for a variation of the *integrated* LDOS (i.e., charge density) throughout the particle core as well.

Keeping the same division of the inner core, we can try in a next step to model the surface metal atoms with the second scenario, where we assume that the surface layer has ''metallic'' character, rather than ''nonmetallic.'' Accordingly, we assume a single *IS* value, identical for each surface site, determined from the fitting to the data, leaving free the *QS* for each site. From the cuboctahedral cluster shape, we find the following surface sites (see Fig. 2): 12 atoms at the corners (c), 24 atoms on the triangular {111} surfaces (t), 54 atoms on the square {001} surfaces (s_1,s_2,s_3), and 72 atoms on the edges (e_1,e_2: intersections between {111} and {001} surfaces). The resulting fit, plotted in Fig. 7(d) (Table III), is of the same quality as that in Fig. 7(c), and has an *IS* well below 2 mm/s, as expected for Au atoms participating in a delocalized electron system. Apparently, it is not necessary to assume a ''nonmetallic'' surface layer, in which atoms bonded to ligands are monovalent, and unligated atoms pentavalent. Especially the latter valence appears to be an unphysical result, since it seems very unlikely that unbonded sites would have a higher valence than bonded ones. Contrastingly, it seems much more likely that the surface layer is part of the delocalized electron system of the metal core, and this assumption fits the data just as well. Careful examination of the resulting *QS* values (Table III) shows that they increase for the different sites, with a decreasing number of nearest neighbors (see Table II). As we shall see below, all clusters show this same systematic correlation. We will come back to these points in Sec. VI. Of course, we do not want to claim that the *IS* and *QS* in reality do not depend on the ligation at all. However, it appears that these parameters depend more on the local metal-atom coordination than on the type of ligand, and that their correlation indicates a larger degree of delocalization at the surface metal atoms than was

previously[21,22] suggested. Still, it would be desirable to have additional information from other experiments or from more sophisticated calculations.

We next turn to data on another four-shell Pt cluster with a different ligand shell, namely, the Pt4cinc compound, for which a spectrum was recorded at $T=4.2$ K. The chemical composition of this compound shows that there are many more ligands present than can be accommodated at the surface of a Pt4 particle. This hampers a judicious guess for the ligand structure, and thus we have to turn to a more simplified approach. We may again first assume that all surface sites have the Au atom in a definite valence state, with a *QS*-*IS* pair that exactly matches one of the correlation lines for the mono-, tri-, or pentavalent Au states, as used above for Pt4phen*. Since the numbers of atoms in each valence state are not known, we leave the relative intensities *I* for the surface sites as free parameters, whereas *I* for the core sites is set to the calculated values (using the bulk force constants, cf. Table II), which fixes the total spectral weight for the surface as well. The core *IS* and θ_D^{inter} were left as free fitting parameters. The best fit was obtained with a surface consisting solely of Au^I and Au^V, presented in Fig. 8(a) and Table IV. The relative weights of Au^I and Au^V in the surface are remarkably similar to those found for Pt4phen*. Apparently, the spectral contribution of the surface is very similar in both. Since the ligands are completely different, this implies that the shape of the surface spectral contribution is indeed mainly caused by the geometric structure of the surface of the Pt4 particle, instead of by the type of ligand, which is in accordance with the interpretation that we believe to be most likely, namely, that the surface layer remains part of a delocalized electron system.

Just as in Pt4phen*, the mismatch between the fit and the data around the peak produced by the inner core [see the difference plot of Fig. 8(a)] is a strong indication for an *IS* value varying throughout the core. Figure 8(b) shows a fit with two core sites, one containing the inner 55 atoms, and one containing those in the third shell. Just as for Pt4phen*, this fit is excellent, which we interpret as additional evidence that the electron density varies throughout the core.

Finally, Fig. 8(c) shows a fit assuming a ''metallic'' surface, with a single *IS* for all surface sites, and a value of *QS* depending on the geometric location on the particle surface. The result is of the same quality as in Fig. 8(b). Again, we find an *IS* below 2 mm/s, and a *QS* that increases with a decreasing number of nearest neighbors (cf. Tables II and IV).

The result for θ_D^{inter} in all fits to the Pt4cinc data (approximately 8 K) is much lower than for Pt4phen* (15 K), which means that the matrix in which the metal particles are embedded is much softer. The presence in the matrix of 369 acetate molecules per Pt4 particle, together with 102 cinchonidine ligands, may explain this difference. Many of the molecules are probably not rigidly connected to the Pt4 particles, which may increase their vibrational degrees of freedom, and produce a ''softer'' matrix for the Pt particles.

B. Colloids of Pt and Au particles

For the larger particles, the core contribution itself should be a single peak, with a bulk *IS*. The surface-to-volume ratio becomes very small, so that all surface effects should be less visible than in small particles. Also the QSE should gradually disappear with increasing size. On the basis of such considerations, the colloids form an attractive intermediate between the small molecular metal clusters and the bulk. The surface screening and QSE might still be visible in the Mössbauer spectra, in particular for Pt-c33, and possibly for the intermediate Au-c65 and Au-c66 particles, which contain much smaller particles than Au-c172. However, there is little chance that the surface sites can be resolved so distinctly as in the molecular clusters, moreso since in the colloids there is a small distribution in size and shape of the particles. So, even for Pt-c33, the various different surface sites can probably not be distinguished from each other, as could be done in the Pt4 particles, but the large difference in *f* factors between surface and core sites should remain visible (cf. Table II).

Figures 9 and 10 show the spectra recorded at 4.2 K. The fits on the spectra of all three colloidal Au samples (Fig. 9 and Table V) have a single core site, with an *IS* around the bulk value. There appears to be no need to allow for a varying *IS* through this core, indicating that in Au particles larger than about 6 nm, the QSE and surface screening effects are too small to be resolved. This agrees with the theoretical expectations outlined in Sec. III. For Au-c172, the surface

TABLE IV. Parameters of the fits in Fig. 8. Fixed parameters are indicated by bold faced values. Values of *IS* and *QS* are given in mm/s. *IS* is with respect to ^{197}Au/Pt, and reversed in sign (see text). The relative intensity *I* of the core sites was fixed to the calculated values (Table II). In (a), a single core site was used, whereas in (b) and (c), the core was divided into two contributions. In (a) and (b), the *QS* of the surface sites was calculated from the *IS*, depending on the indicated valency. In (c), the surface sites are assigned, according to the local metal-atom coordination (cf. Fig. 2), *I* for all sites is taken from Table II, and only a single *IS* value was used to fit all surface sites.

Pt4cinc (a), $\chi^2_{red}=1.78$	*IS*	*QS*	*I* (%)
Core 0–3	0.19		**60**
Surface	1.5	Au^I	15
Surface	1.8	Au^V	25
Pt4cinc (b), $\chi^2_{red}=1.30$			
Core 0–2	−0.40		**23**
Core 3	0.51		**37**
Surface	1.5	Au^I	16
Surface	1.8	Au^V	24
Pt4cinc (c), $\chi^2_{red}=1.27$			
Core 0–2	−0.40		**23**
Core 3	0.65		**37**
Corner (c)	1.8	9.6	**2**
Edge (e_1,e_2)	1.8	6.2	**16**
Square (s_1,s_2,s_3)	1.8	1.1	**15**
Triangle (t)	1.8	0.1	**7**

TABLE V. Parameters of the fits in Fig. 9, using a single core site and one or two surface sites. Fixed parameters are indicated by bold faced values. *IS* was kept constant over the surface in the latter case. *N* is the *relative* site occupancy, since the total number of atoms is not known. Values of *IS* and *QS* are given in mm/s. *IS* is with respect to ^{197}Au/Pt. See the text for more information.

Au-c65, $\chi^2_{red}=1.14$	*IS*	*QS*	*I* (%)	*N* (%)	f^{intra}
Core	−0.05		**81**	**76**	**0.189**
	1.1	**0.0**	14	18	**0.14**
	1.1	3.8	5	6	**0.14**
Au-c66, $\chi^2_{red}=1.25$					
Core	−0.01		**81**	**76**	**0.189**
	0.9	**0.0**	15	19	**0.14**
	0.9	3.9	4	5	**0.14**
Au-c172, $\chi^2_{red}=1.27$					
Core	0.00		93	**90**	**0.189**
	0.9	1.3	7	**10**	0.14

can be represented by one contribution to obtain a good fit, whereas for Au-c65 and Au-c66, two are needed. In the latter case, the *IS* was forced to be the same for both surface contributions, resulting in a low shift of about 1 mm/s with respect to that in bulk Au. This suggests, as above for the Pt4 particles, that the electrons in the surface layer participate in the delocalized electron system of the whole particle. Due to the distribution in shapes and sizes of the particles, we will not assign any significance to the *QS* values.

Since only two sites are needed to fit the Au-c172 spectrum, the relative intensity of both could be left free as a fitting parameter. In order to relate these to an average surface *f* factor, we need values for the relative number of atoms in that site and for the core *f* factor. We take 9.7% for the relative number of atoms, which equals the fraction of atoms in a monatomic surface layer for a spherical chunk of bulk Au, with a diameter equal to the average diameter of the Au-c172 particles (17.2 nm). If we use for the core *f* factor the bulk value of 0.189, we find from the experiment an average surface *f* factor of 0.14, very similar to what is found for the smaller molecular clusters such as Au2. (See below.) Indeed, also for such a large particle the reduced metal-atom coordination on the particle surface still leads to the same drastic reduction of the *f* factor. For the two smaller colloids, Au-c66 and Au-c65, two sites are needed to represent the surface, the *f* factors of which were fixed to this same value of 0.14. As for Au-c172, the relative surface-to-volume ratio was calculated from the average particle diameters, thus fixing the relative intensity of the core sites. The resulting fits are satisfactory, the small deviations that remain visible in the difference spectra being probably caused by the above-mentioned shape and size distributions, which would lead to an increase of the linewidth of the surface sites.

At variance with the Au colloids, the 3.3-nm Pt-c33 particles have a size close to that of the small magic number

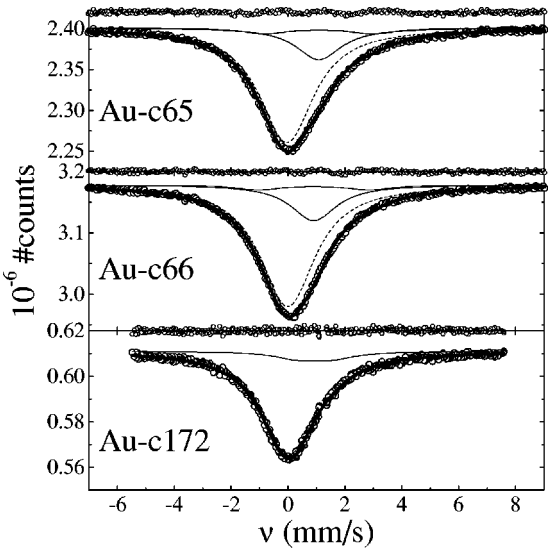

FIG. 9. Spectra on the Au colloids at $T=4.2$ K. Symbols as in Fig. 7. The model is a single core site, with one or two (small) contributions from the surface.

clusters. In fact, the average particle diameter approximately corresponds to that of a six-shell (Pt_{923}) magic number cluster, which would have a corner-to-corner distance of 3.6 nm and a square-face-to-square-face distance of 2.5 nm. The fraction of surface atoms in a Pt sphere with 3.3-nm diameter is still rather high (42%), and it is very close to the 39% surface fraction in a Pt6 cluster. For that reason, we modeled the spectrum of Pt-c33 with that expected for a Pt6 magic number cluster. We assumed a ''metallic'' surface consisting of two sites with an identical *IS*, but different *QS*. Figure 10(a) and Table VI show the resulting fit, assuming a single core site. *f* factors were estimated, based on those found for the Pt4 clusters: 0.22 and 0.14, as averages for the core and for the surface, respectively (cf. Fig. 6, and Table II). However, just as in the single core fits to the Pt4 spectra, the difference plot shows a deviation around the central (core) peak, albeit less pronounced. Adding more surface sites does not improve the fit, but dividing the core into two contribu-

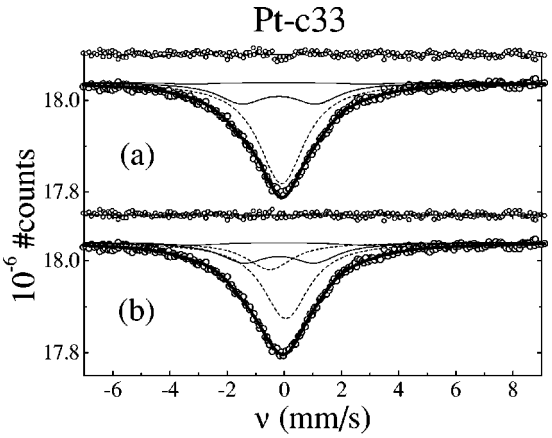

FIG. 10. Two different fits to the same data taken on Pt-c33 at $T=4.2$ K. Symbols as in Fig. 7. (a) Single core site, two surface sites. (b) Two core sites, two surface sites.

TABLE VI. Parameters of the fits in Fig. 10. Fixed parameters are indicated by bold faced values. The spectrum of the Pt-c33 particle was modeled by a Pt6 cluster, with 561 atoms in the core and 362 atoms at the surface. The relative intensity of the core was fixed, and the surface was modeled by two sites with identical *IS*. In (a), a single core site was used, whereas in (b), it was divided into two contributions. *N* is the site occupation, and f^{intra} was fixed to estimated values. Values of *IS* and *QS* are given in mm/s. *IS* is with respect to ^{197}Au/Pt, and reversed in sign (see text).

Pt-c33 (a), $\chi^2_{red}=1.69$	*IS*	*QS*	*I* (%)	*N*	f^{intra}
Core 0–5	0.09		**71**	**561**	**0.22**
	0.19	6.1	2	25	**0.14**
	0.19	2.6	27	337	**0.14**
Pt-c33 (b), $\chi^2_{red}=1.43$					
Core 0–3	0.52		**19**	**147**	**0.22**
Core 4,5	−0.05		**52**	**414**	**0.22**
	0.18	6.2	4	51	**0.14**
	0.18	2.5	25	311	**0.14**

tions, with different *IS*, results in the fit shown in Fig. 10(b) (Table VI), which is clearly better. The core was again divided into two sites, one containing shells zero to three, and the other shells four and five. Thus, the Pt colloid appears to be still small enough to give a detectable variation of the electron density in the core, attributed to QSE and/or surface screening effects. The *IS* of the two surface sites can be taken as identical, resulting in values low enough to correspond to a ''metallic'' surface layer.

The conclusions on the varying core *IS* in Pt-c33, and on the character of the surface of the Au and Pt colloids should be taken with care, since the fitted surface sites just reproduce the shape of the surface spectral contribution, and do not uniquely represent the large number of physically different sites in the assembly of colloidal particles, with shape and size distributions. However, the surface spectral contribution is apparently rather symmetric, in accordance with a constant *IS* for all surface sites, and its value is rather low, as expected for a ''metallic'' surface. We therefore conclude that the electron density in the core of 3-nm Pt particles may still be influenced by surface screening and QSE, whereas for Au particles larger than 6 nm, these effects are too small to be resolved. Furthermore, the surface shell of the Pt and Au colloids most probably is part of the delocalized electron system, as for the above presented Pt4 clusters.

C. Two-shell $Au_{55}(PPh_3X)_{12}Cl_6$ and $Pt_{55}(AsBu_3)_{12}Cl_{20}$ clusters, and $Pt_{38}(CO)_{44}$ clusters

The Pt and Au colloids thus appear to present very useful intermediates between the four-shell Pt_{309} clusters and the bulk. In the opposite direction, towards smaller clusters, an excellent series of clusters to test the models described in this paper are the two-shell Au and Pt clusters, and the even smaller Pt_{38} cluster. The Au2tpp cluster compound has been investigated by Smit *et al.*,[20] followed by more extensive studies on several Au2 clusters with other ligands by Mulder *et al.*,[21] and van de Straat *et al.*[23] As a typical example Fig. 11 shows the spectrum on Au2tpp recorded by Mulder *et al.* at $T=4.2$ K, with the corresponding fit. This spectrum is also representative for the Au2 clusters with other ligands, except for a water soluble version[23] which will not be discussed here. The distinct structure of the spectrum allows for independent fitting, not only of the *IS* and *QS*, but also of the relative intensity *I* for each site. In a two-shell cuboctahedral particle, there are five geometrically different sites (cf. Fig. 2 and Table II): 1 central atom, 12 atoms in the first (inner) shell, and 42 in the second (surface) shell, of which 12 atoms are on the corners (c), 24 on the edges (e), and 6 in the center of each square (s, {001} planes). In all Au2 compounds studied,[20,21,23] the ligand shell is composed of 12 molecules of a PPh_3 derivative (see Fig. 3), the type varying with the compound, and in addition six Cl atoms. These ligands are expected to be connected to the corners (c) and to the squares (s), respectively, which is likewise the geometric site assignment of the surface metal atoms. X-ray[68] and EXAFS[14] studies on Au2tpp revealed an fcc structure, with a lattice contraction relative to bulk Au of about 3–4 %, accompanied by a considerable decrease of the vibration factor compared to the bulk, and thus by a lattice stiffening of the particle. The central atom and the first shell were taken to have identical Mössbauer parameters, represented by a single core site (dashed line in Fig. 11). Since the number of atoms participating in each site is given by the structure, the total intensity of each site is a direct measure for the effective *f* factors.

Mulder *et al.*[21] found zero *QS* in the inner core, confirming the cubic fcc structure. After correcting the measured $IS=-1.44$ mm/s for the volume reduction due to the lattice contraction (from $\delta IS/\delta \ln V=-6$ mm/s, the correction is $\delta IS\approx -0.6$ mm/s), one obtains $IS_{corr}\approx -2.0$ mm/s, which deviates by about -0.8 mm/s from the bulk Au value (-1.22 mm/s). This deviation was attributed to charge transfer to the surface atoms, as well as further charge transfer to the ligands. The *IS* of all surface sites for three differently ligated Au2 particles varies between -0.2 and 1.0 mm/s.[21] The *QS-IS* pairs were located near the Au^I region for the ligand-bonded sites, and near the Au^{III} region for the unbonded (bare) sites (see also Fig. 4). The evolution of the intensity of the lines with temperature between 1.5 and 30 K was translated into a temperature dependence of the *f* factors for each site separately, which could be fitted with the central

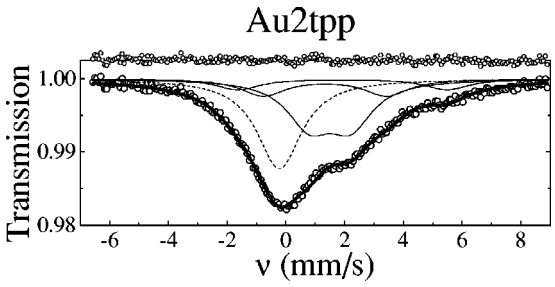

FIG. 11. Data taken from Mulder *et al.* (Ref. 21) on Au2tpp at $T=4.2$ K. Symbols as in Fig. 7.

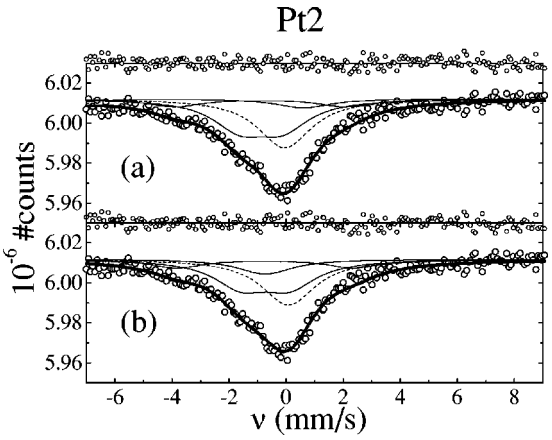

FIG. 12. Two different fits to the same data taken on Pt2 at $T=4.2$ K. Symbols as in Fig. 7. (a) Single core site, nonmetallic surface. (b) Single core site, metallic surface.

force model, resulting in values of $\theta_D^{inter}=15$ K, and $C_{\text{Au-Au}}=30$ N/m, for Au2tpp. The f factors of the surface atoms were found to be strongly reduced, compared to the inner core, reflecting their reduced metal atom coordination.

We can now compare the previously derived force constant for Au2tpp with the here-obtained bulk value. The volume contraction of the cluster, compared to the bulk, would lead to a considerable increase of the bulk modulus,[14] and thus of the force constant, $C_{\text{Au-Au}}$. As argued in Sec. IV, a reliable value for modeling the f factors in the bulk is $C_{\text{Au-Au}}^{bulk}=25.0(6)$ N/m. The experimentally observed $C_{\text{Au-Au}}=30$ N/m, deduced from f^{intra} of all Au atoms in the Au2tpp clusters, is indeed considerably larger, confirming the volume reduction in these particles. The other Au2 clusters, which were not investigated by EXAFS, were found to give the same $C_{\text{Au-Au}}$ value,[21] from which we conclude that they have a contracted metal core as well.

From the observation that all *QS*-*IS* pairs for the surface sites fall in the regions for Au^I and Au^{III}, one might infer that the surface layer of the Au2 particles is ''nonmetallic.'' However, just as for the ''Au^V sites'' in the Pt_4 clusters, a strong objection against such an interpretation is that it is very unlikely that the unbonded surface sites (here Au^{III}) would be oxidized even further than the bonded ones (Au^I). Furthermore, it is noteworthy that the values of *IS* on the surface of all Au2 clusters roughly lie between 0 and 1 mm/s, whereas the *QS* varies from 0 to 7 mm/s (see plus symbols in Fig. 4). In the case of the Pt4 particles, we used a single *IS* value for the whole surface, at a value below 2 mm/s, and different *QS* values for geometrically different sites, to represent the ''metallic'' character of the surface layer. Since the geometric surface site assignment in Au2 particles is the same as that according to the ligands bonded to the surface atoms, the situation in Au2 particles appears to be very similar to that in the Pt4 particles. Therefore, the previously found similar *IS* values (between 1 and 2 mm/s) for the different surface sites of Au2 particles should in our opinion be interpreted as evidence for a delocalized electron system at the surface layer, with again the least coordinated surface sites having the highest *QS* values. (See Sec. VI.)

TABLE VII. Parameters of the fit in Fig. 12. Fixed parameters are indicated by bold faced values. *I* is taken from Table II. In (a), the *QS* of the surface sites was calculated from the *IS* depending on the indicated valency. In (b), only a single value for *IS* was used for all surface sites. Values of *IS* and *QS* are given in mm/s. *IS* is with respect to ^{197}Au/Pt, and reversed in sign (see text).

Pt2 (a), $\chi^2_{red}=1.03$	*IS*	*QS*	*I* (%)
Core 0,1	0.05		**36**
Corner	4.1	Au^I	**13**
Edge	0.9	Au^{III}	**40**
Square	0.9	Au^I	**11**
Pt2 (b), $\chi^2_{red}=1.18$			
Core 0,1	0.06		**36**
Corner	0.7	6.2	**13**
Edge	0.7	1.7	**40**
Square	0.7	0.2	**11**

As in the Pt4 clusters, the absence of a *QS* in the inner core of the Au2 clusters is in agreement with cubic packing. For the whole Au2 series, the average corrected *IS* of the core deviates from the bulk value by -1 mm/s. This may indeed be related to electron transfer to the ligands, or to other effects described above, namely, surface screening and QSE. A variation of the *IS* throughout the core would be hardly observable in this case, as there are 12 identical atoms with the same distance to the surface and only one central atom with a different distance. This ratio is too large to resolve the single central atom from the spectrum, although a different *IS* for this atom might explain the small remaining deviation between fit and data around -1 mm/s. At any rate, the fact that the *IS* values for the inner core are so close for all different Au2 clusters confirms our assumption that a lattice contraction as observed for Au2tpp is probably present in all these compounds.

The spectrum of the Pt2 cluster compound at $T=4.2$ K is displayed in Fig. 12. Fits were made using the ''metallic'' and ''nonmetallic'' surface models (see Table VII), as in the Pt4 clusters. We took only one site to represent the 13-atom core, as in the Au2 clusters. f factors were again calculated using the bulk force constants. The surface consists of three sites with different local symmetry (cf. Fig. 2 and Table II): 12 atoms on the corners (c), 24 on the edges (e), and 6 in the center of the squares (s). The distribution of the ligands over the surface is assumed not to change this site assignment, just as in Au2. There are 12 $AsBu_3$ ligands, probably located at all corners, and 20 Cl atoms. The latter are probably distributed as homogeneously as possible over the remaining surface: one on the center of each triangle (in total 8 Cl atoms) and two on each square (in total 12 Cl). Assuming first a ''nonmetallic'' surface layer, we can try several combinations for the valence states of the surface sites and see which one fits best. The best fit, shown in Fig. 12(a), gives Au^I for the $AsBu_3$ ligated corner sites, Au^{III} for the edges, and again Au^I for the square {001} faces. The core *IS* $=0.05$ mm/s, close to the bulk value 0.00. The difference

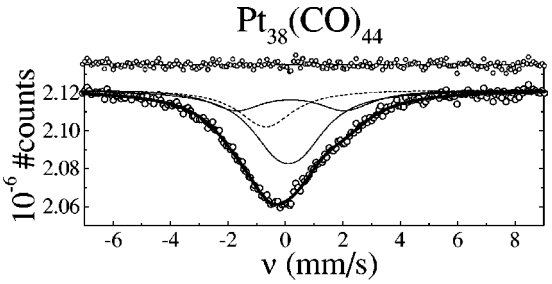

FIG. 13. Pt_{38} at $T=4.2$ K. Symbols as in Fig. 7. $\theta_D^{inter}\approx 45$ K. See the text for more detailed information.

may be attributed, as in Au2, to the possibly combined effects of charge transfer to the ligands, surface screening, and the QSE.

Figure 12(b) shows the fit assuming a ''metallic'' surface with an *IS* identical for all surface atoms. Again, a correlation of the *QS* with the number of nearest neighbors is found (cf. Table II). Unfortunately, the statistics in these data are not good enough to allow us to decide if this model is better than the ''nonmetallic'' surface model, although χ^2 values indicate a small preference for the latter, and again the values of *IS* are low for all surface atoms, except those at the corners. This may indicate that the delocalized electron system extends over all Pt atoms, except those at the corners.

Data for the smallest cluster discussed here, Pt_{38}, have been reported before by van de Straat *et al.*[23] We reinterpret the spectra, using the new bulk force constants derived in the central force model (cf. Table II). The result for the $T=4.2$ K spectrum is shown in Fig. 13, with a three-site fit (see Table VIII). The choice of sites is unambiguous in this case, since the molecular crystal structure is completely known.[7] The inner core consists of six crystallographically identical atoms, whereas there are only two different sites at the surface (cf. Figs. 1 and 2): 24 atoms at corners (c) and 8 atoms at the center of hexagons (h). All 32 surface atoms have a CO molecule as a ligand. In addition, there are 12 CO molecules bridging every two corner atoms. The site assignment thus remains unaltered by the ligands. As said above, most of the Pt-Pt distances deviate at most by 1% from the bulk value.

In these crystals, there are also two singly ionized tetraphenyl-phosphine $(PPh_4)^+$ molecules present per Pt_{38} unit, which charge the latter to $-2e$. The Coulomb forces, responsible for the intermolecular bonds, are thus expected to be much stronger than the van der Waals forces that bind the other investigated clusters into a molecular solid. The temperature dependence of the measured f^{inter} between 4.2 and 60 K was fitted using the Debye model, leading to $\theta_D^{inter}\approx 45$ K, which is indeed much larger than that found for the Au2 (15–19 K)[21] and Pt4 particles (8–15 K, see Sec. V A). However, in this case, the experimental $f^{inter}(T)$ is not very well represented by such a fit (see also Ref. 23), which may indicate the breakdown in this ionic solid of the possibility to write the total *f* factor in terms of a product of f^{intra} and f^{inter}.

TABLE VIII. Parameters of the fit in Fig. 13, using a single core site and a single surface site. Fixed parameters are indicated by bold faced values. *I* is taken from Table II. Values of *IS* and *QS* are given in mm/s. *IS* is with respect to ^{197}Au/Pt, and reversed in sign (see text).

Pt_{38}, $\chi^2_{red}=1.35$	*IS*	*QS*	*I* (%)
Core	0.68		**23**
Corner	−0.18	3.79	**25**
Hexagonal center	−0.11	0.86	**52**

Since the cluster geometry and the ligand coordination is completely known, this Pt_{38} particle forms an ideal system to test our two scenarios for modeling the surface sites. In the fit presented in Fig. 13, all *IS* and *QS* values were left free, except that we fixed, as before, $QS=0$ in the core. It is striking to see that the *IS* of both surface sites, which are now definitely known to be the (c) and (h) sites, is almost the same and has a low value of about -0.1 mm/s. This indicates delocalized electrons, and an almost constant electron density over the surface, which we have interpreted as a strong indication for a ''metallic'' surface. If the surface would be ''nonmetallic,'' the different ligand coordination of (c) and (h) sites would most probably cause a different charging of both sites, resulting in different and larger *IS* values. So we conclude that, even in this very small particle, all Pt atoms appear to be part of a delocalized electron system, characteristic of a metal. Again, the least coordinated site (cf. Table II) has the highest *QS*, confirming the tendency observed in the other particles. The core *IS* $=0.68$ mm/s, which may again be attributed to charge transfer with the ligands, and in this case also with the PPh_4 molecules, or to surface screening or QSE.

VI. SUMMARY AND CONCLUSIONS

We have presented and analyzed in this paper the collected results of an extensive ^{197}Au Mössbauer spectroscopic investigation on a series of Pt and Au metal nanoparticles of varying sizes. On the one hand, a series of molecular clusters is involved, which allows a detailed analysis of the contribution of the various sites in the inner core and on the surface of the particles. On the other hand, related Pt and Au colloids were available, which generally have a larger volume and thus form an attractive intermediate between the molecular nanoclusters and the bulk.

The physical properties that can be probed by Mössbauer spectroscopy are the electronic configuration and the vibrational modes. The electronic properties in small metal particles are expected to be influenced drastically by the small size. Confining free electrons to a small particle results in an oscillatory behavior of the electron density due to the QSE. A large surface-to-volume ratio produces a large contribution from the surface, so that all kinds of surface effects become important as well. Near to a metal surface, the electron density fluctuates due to screening of the surface (Friedel oscillations). These fluctuations, together with those from the QSE, are expected to produce a net variation of the *IS* inside the metal cores of the molecular clusters, which we have been able to confirm experimentally. The deviations between

data and fits that do not take into account such oscillations decrease gradually with increasing particle size, in agreement with theoretical expectation that the amplitude of the fluctuations should decrease with increasing size. Au and Pt particles, with diameters up to 4 nm, do show the fluctuations, whereas Au particles with a diameter larger than 6 nm do not. The average *IS* values in the inner core of the particles do not show any clear correlation with the particle size, except that in the Au colloids it is almost the same as in the bulk, whereas in all the other particles it deviates slightly (less than 1 mm/s) from the corresponding bulk values. This may be due to surface screening and QSE, or to charge transfer with the different ligands, having varying degrees of electron acceptance.

In the monatomic surface layer of metal atoms, many effects play a role in the values of *IS* and *QS*. We have argued that these effects can be treated using the concept of a local density of states (LDOS). A tight-binding analysis then shows that the local metal-atom coordination has a dominant effect on the *QS* and *IS* for the various sites on a ''metallic'' surface, which we defined as one that is part of the volume over which electrons are delocalized, so that free charge exchange is possible between such a ''metallic'' surface and the rest of the metal particle. This results in, among others, surface level shifts[48] that depend strongly on the number of nearest neighbors of a surface atom. Variations in *QS* can then be quite large, whereas those in *IS* are expected to be much less pronounced. Furthermore, delocalized bonds in very small Au clusters usually result in low values of the *IS*. The local symmetry at a surface site is another important aspect that can have a large influence on the value of the *QS*.

All metal nanoparticles are stabilized by ligands, to prevent them from coalescing. These ligands may have a variety of effects. First of all, they will act as electron donors or acceptors, thus charging the metal core and changing its average *IS*. Furthermore, they interact directly with the surface metal atoms, which may influence their *QS* and *IS* values. If the surface layer would be ''nonmetallic,'' atoms in that layer may accumulate some charge, so that they would resemble atoms in a certain valence state, as in insulating monatomic Au complexes. The *QS* and *IS* then would become reminiscent of Au^{I}, Au^{III}, or Au^{V}. We have shown that this approach systematically leads to unphysical results for the valence states, namely, a higher oxidation state for unligated surface atoms than for ligated surface atoms. On the other hand, assuming a ''metallic'' surface layer, with a single value of *IS* over the whole surface, leads to good fits in all cases presented, and to very low *IS* values, from which we conclude that the surface layer remains part of the delocalized electron system, characteristic of a metal, even for metal particles down to a size of only 38 atoms. An interesting feature that emerged is that the *QS* value of a surface site is strongly correlated *with the local metal-atom coordination*. The number of nearest neighbors has a large influence on surface level shifts, but this cannot fully explain the variation of *QS*. Another important factor will be the symmetry of the local coordination of the metal atom. In our cuboctahedral molecular clusters, as well as in Pt_{38}, this symmetry becomes more and more cubic with an increasing number of nearest neighbors. From insulating monatomic Au complexes, we know that *QS* is generally higher for compounds with a less cubic coordination of the Au atom. (The *QS* decreases in the series Au^{I}, Au^{III}, Au^{V}.) This may be related to the observed correlation. Obviously, more detailed theoretical calculations would be very welcome for a full account of the experimentally observed strong and systematic variations.

*Corresponding author. Email address: DeJongh@Phys.LeidenUniv.nl

[1] *Clusters and Colloids, From Theory to Applications*, edited by G. Schmid (VCH, Weinheim, 1994).

[2] *Metal Clusters in Chemistry*, edited by P. Braunstein, L. A. Oro, and P. R. Raithby (Wiley-VCH, Weinheim, 1999).

[3] A. Züttel, Ch. Nützenadel, G. Schmid, and F. Fauth (private communication).

[4] R. E. Benfield, A. Filipponi, D. T. Bowron, R. J. Newport, and S. J. Gurman, J. Phys. C **6**, 8429 (1994).

[5] R. E. Benfield, A. Filipponi, D. T. Bowron, R. J. Newport, S. J. Gurman, and G. Schmid, Physica B **208&209**, 671 (1995).

[6] We mention that Moiseev and co-workers [see M. N. Vargaftik, V. P. Zagorodnikov, I. P. Stolarov, I. I. Moiseev, D. I. Kochubey, V. A. Likholobov, A. L. Chuvilin, and K. I. Zamaraev, J. Mol. Catal. **53**, 315 (1989)] have obtained several forms of Pd5, with differences not only in the ligand shells, but also different with respect to the atomic packing inside the metal core (fcc or icosahedral).

[7] A. Ceriotti, P. Chini, G. Longoni, D. M. Washecheck, E. J. Wucherer, and L. F. Dahl, in *XIII Congresso Nazionale di Chimica Inorganica*, Camerino, Italy, September 23–26, 1980, p. A2.

[8] M. P. A. Viegers nad J. M. Trooster, Phys. Rev. B **15**, 72 (1977).

[9] L. Stievano, S. Santucci, L. Lozzi, S. Calogero, and F. E. Wagner, J. Non-Cryst. Solids **232-234**, 644 (1998).

[10] Y. Kobayashi, S. Nasu, S. Tsubota, and M. Haruta, Hyperfine Interact. **126**, 95 (2000).

[11] *Physics and Chemistry of Metal Cluster Compounds*, edited by L. J. de Jongh (Kluwer, Dordrecht, 1994).

[12] G. Pacchioni and N. Rösch, Inorg. Chem. **29**, 2901 (1990).

[13] N. Rösch, L. Ackermann, and G. Pacchioni, J. Chem. Phys. **95**, 7004 (1991).

[14] M. A. Marcus, M. P. Andrews, J. Zegenhagen, A. S. Bommannavar, and P. Montano, Phys. Rev. B **42**, 3312 (1990).

[15] H. H. A. Smit, R. C. Thiel, and L. J. de Jongh, Z. Phys. D: At., Mol. Clusters **12**, 193 (1989).

[16] P. D. Cluskey, R. J. Newport, R. E. Benfield, S. J. Gurman, and G. Schmid, Z. Phys. D: At., Mol. Clusters **26**, S8 (1993).

[17] R. E. Benfield, A. Filipponi, N. Morgante, and G. Schmid, J. Organomet Chem. **573**, 299 (1999).

[18] Y. Volokitin, J. Sinzig, L. J. de Jongh, G. Schmid, M. N. Vargaftik, and I. I. Moiseev, Nature (London) **384**, 621 (1996).

[19] F. C. Fritschij, H. B. Brom, L. J. de Jongh, and G. Schmid, Phys. Rev. Lett. **82**, 2167 (1999).

[20] H. H. A. Smit, P. R. Nugteren, R. C. Thiel, and L. J. de Jongh, Physica B **153**, 33 (1988).

[21] F. M. Mulder, R. C. Thiel, L. J. de Jongh, and P. C. M. Gubbens, Nanostruct. Mater. **7**, 269 (1996).
[22] F. M. Mulder, T. A. Stegink, R. C. Thiel, L. J. de Jongh, and G. Schmid, Nature (London) **367**, 716 (1994).
[23] D. A. van de Straat, R. C. Thiel, L. J. de Jongh, P. C. M. Gubbens, G. Schmid, A. Ceriotti, and R. della Pergola, Z. Phys. D: At., Mol. Clusters **40**, 574 (1997).
[24] For a review, see J. J. van der Klink and H. B. Brom, Prog. Nucl. Magn. Reson. Spectrosc. **36**, 89 (2000).
[25] R. V. Parish, in *Mössbauer Spectroscopy Applied to Inorganic Chemistry*, edited by G. J. Long (Plenum, New York, 1984), Vol. 1.
[26] H. D. Bartunik, W. Potzel, R. L. Mössbauer, and G. Kaindl, Z. Phys. **240**, 1 (1970).
[27] J. S. Charlton and D. I. Nichols, J. Chem. Soc. A 1484 (1970).
[28] M. P. A. Viegers, Ph.D. thesis, Katholieke Universiteit Nijmegen, 1976.
[29] O. D. Häberlen, S.-C. Chung, M. Stener, and N. Rösch, J. Chem. Phys. **106**, 5189 (1997).
[30] H. Häkkinen, R. N. Barnett, and U. Landman, Phys. Rev. Lett. **82**, 3264 (1999).
[31] N. N. Greenwood and T. C. Gibb, *Mössbauer Spectroscopy* (Chapman and Hall, London, 1971).
[32] D. J. Erickson, L. D. Roberts, J. W. Burton, and J. O. Thomson, Phys. Rev. B **3**, 2180 (1971).
[33] S. Margulies and J. R. Ehrman, Nucl. Instrum. Methods **12**, 131 (1961).
[34] N. D. Lang and W. Kohn, Phys. Rev. B **1**, 4555 (1970).
[35] N. D. Lang and A. R. Williams, Phys. Rev. B **18**, 616 (1978).
[36] S. Sugano, *Microcluster Physics* (Springer-Verlag, Berlin, 1991), Chap. 3.
[37] W. D. Knight, K. Clemenger, W. A. de Heer, W. A. Saunders, M. Y. Chou, and M. L. Cohen, Phys. Rev. Lett. **52**, 2141 (1984).
[38] W. A. de Heer, W. D. Knight, M. Y. Chou, and M. L. Cohen, *Electronic Shell Structure and Metal Clusters*, *Solid State Physics* (Academic, New York, 1987).
[39] M. Brack, Rev. Mod. Phys. **65**, 677 (1993).
[40] R. P. Messmer, S. K. Knudson, K. H. Johnson, J. B. Diamond, and C. Y. Yang, Phys. Rev. B **13**, 1396 (1976).
[41] R. Haydock and M. J. Kelly, Surf. Sci. **38**, 139 (1973).
[42] G. Pacchioni, S. Krüger, and N. Rösch, in Ref. 2, Sec. 4.6.
[43] A. Zangwill, *Physics at Surfaces* (Cambridge University Press, Cambridge, England, 1988), Chap. 4.
[44] A ''healing-length'' model for the local density of states was also used to explain the strong size dependence of the magnetic susceptibility of the series of (magic number) Pd cluster compounds and colloids: D. A. van Leeuwen, J. M. van Ruitenbeek, G. Schmid, and L. J. de Jongh, Phys. Lett. A **170**, 325 (1992).
[45] H. E. Rhodes, P.-K. Wang, H. T. Stokes, C. P. Slichter, and J. H. Sinfelt, Phys. Rev. B **26**, 3559 (1982).
[46] C. D. Makowka, C. P. Slichter, and J. H. Sinfelt, Phys. Rev. B **31**, 5663 (1985).
[47] P. H. Citrin and G. K. Wertheim, Phys. Rev. B **27**, 3176 (1983).
[48] What we call a surface level shift is better known in the literature as the surface *core*-level shift. However, since we are interested in the shifts and other changes around the Fermi level, we prefer to drop the word ''core'' here.
[49] G. K. Shenoy and F. E. Wagner, *Mössbauer Isomer Shifts* (North-Holland, Amsterdam, 1978), p. 906.
[50] J. E. Inglesfield, in *Interactions of Atoms and Molecules with Solid Surfaces*, edited by V. Bortolani, N. H. March, and M. P. Tosi (Plenum Press, New York, 1990).
[51] P. A. Montano, G. K. Shenoy, E. E. Alp, W. Schulze, and J. Urban, Phys. Rev. Lett. **56**, 2076 (1986).
[52] P. Joyes, *Les Agrégats Inorganiques Élémentaires* (Les Editions de Physique, Les Ulis, 1990), Chap. IV.3.
[53] D. A. van Leeuwen, J. M. van Ruitenbeek, L. J. de Jongh, A. Ceriotti, G. Pacchioni, O. D. Häberlen, and N. Rösch, Phys. Rev. Lett. **73**, 1432 (1994).
[54] R. V. Parish, L. S. Moore, A. J. J. Dens, D. M. P. Mingos, and D. J. Sherman, J. Chem. Soc. Dalton Trans. 781 (1988).
[55] L. S. Moore, R. V. Parish, S. S. D. Brown, and I. D. Salter, J. Chem. Soc. Dalton Trans. 2333 (1987).
[56] R. V. Parish, L. S. Moore, A. J. J. Dens, D. M. P. Mingos, and D. J. Sherman, J. Chem. Soc. Dalton Trans. 539 (1989).
[57] N. Nishiguchi and T. Sakuma, Solid State Commun. **38**, 1073 (1981).
[58] H. Wegener, *Der Mössbauereffect* (Hochschultaschenbücher-Verlag, Mannheim, 1966).
[59] The net result of the interparticle vibrations is a reduction of the integrated intensity of the spectrum, especially at temperatures above θ_D^{inter}. However, the total number of emitted photons is conserved, so the loss in intensity of the Mössbauer transition should be compensated by an increase of intensity somewhere else in the spectrum. M. Hayashi, E. Gerkema, A. V. van der Kraan, and I. Tamura, Phys. Rev. B **42**, 9771 (1990). For the particles under present investigation only for the Au-c172 particles is the mass large enough to make the energy shift by the recoil of the whole particle comparable to the natural linewidth, so that this contribution might be visible as a broad Gaussian. However, we did not find evidence for such a contribution in the spectrum (see Sec. V B).
[60] A. Einstein, Ann. Phys. (Leipzig) **34**, 170 (1911).
[61] H. Siethoff and K. Ahlborn, J. Appl. Phys. **79**, 2968 (1996).
[62] N. W. Ashcroft and N. D. Mermin, *Solid State Physics*, International edition (Saunders, Philadelphia, 1976).
[63] P. M. Paulus, Ph.D. thesis, Leiden University, 2000.
[64] H. H. A. Smit, Ph.D. thesis, Leiden University, 1988.
[65] J. Baak, H. B. Brom, L. J. de Jongh, and G. Schmid, Z. Phys. D: At., Mol. Clusters **26**, S30 (1993).
[66] Y. E. Volokitin, Ph.D. thesis, Leiden University, 1997.
[67] J. Baak, Ph.D. thesis, Leiden University, 1993.
[68] M. C. Fairbanks, R. E. Benfield, R. J. Newport, and G. Schmid, Solid State Commun. **74**, 431 (1990).